

Report No. K-TRAN: KSU-97-6  
FINAL REPORT

## **ESTIMATION OF ASPHALT PAVEMENT LIFE**

Mustaque Hossain, Ph.D., P.E.  
Zhong Wu

Kansas State University  
Manhattan, Kansas



JANUARY 2002

**K-TRAN**

A COOPERATIVE TRANSPORTATION RESEARCH PROGRAM BETWEEN:  
KANSAS DEPARTMENT OF TRANSPORTATION  
KANSAS STATE UNIVERSITY  
THE UNIVERSITY OF KANSAS

<b>1 Report No.</b> KTRAN: KSU-97-6	<b>2 Government Accession No.</b>	<b>3 Recipient Catalog No.</b>	
<b>4 Title and Subtitle</b> ESTIMATION OF ASPHALT PAVEMENT LIFE		<b>5 Report Date</b> January 2002	<b>6 Performing Organization Code</b>
		<b>8 Performing Organization Report No.</b>	
<b>7 Author(s)</b> Mustaque Hossaine, Ph.D., P.E., and Zhong Wu, Kansas State University		<b>10 Work Unit No. (TRAIS)</b>	
<b>9 Performing Organization Name and Address</b> Kansas State University 2118 Fiedler Hall Manhattan, Kansas 66506-5000		<b>11 Contract or Grant No.</b> C965	
		<b>13 Type of Report and Period Covered</b> Final Report July 1996 - April 1999	
<b>12 Sponsoring Agency Name and Address</b> Kansas Department of Transportation Bureau of Materials and Research, Research Unit 2300 Southwest Van Buren Street Topeka, Kansas 66611-1195		<b>14 Sponsoring Agency Code</b> RE-0103-01	
		<b>15 Supplementary Notes</b> For more information write to address in block 9.	
<b>16 Abstract</b> <p>The milling of asphalt concrete (AC) pavement surface refers to the mechanical removal of a part of the pavement surface. The Kansas Department of Transportation (KDOT) and the Kansas Turnpike Authority (KTA) routinely mill the surfaces of some AC pavements before inlaying. KTA has adopted a strategy of recycling the upper pavement layer on a relatively frequent basis (every six or seven years) to maintain a smooth riding surface for the last decade or so. However, in most cases, the milling depth is selected based on the rule-of-thumb or experience of the agency for a specific surface distress, such as rutting or transverse cracking, rather than based on any engineering analysis.</p> <p>In this report, the structural and functional performances of such mill-and-inlay AC pavements were analyzed for six different routes of KDOT and KTA. All test sections were tested with the Falling Weight Deflectometer (FWD) at 50 to 100 feet intervals before milling, after milling, and after inlaying. Ten six-inch wide, eighteen-inch long, full-depth asphalt concrete beams were sawn from four test sections. Fatigue tests were conducted in a third-point flexural loading fashion on those field beams sawn into fatigue test specimens of size: 4-in. wide, 3-in. deep and 16-in. long. Distress models and rational transfer factors were found through the analysis of fatigue test results, deflection data, and historical traffic data to estimate the fatigue damage, functional performance, and rutting susceptibility of the mill-and-inlay pavements. For high traffic pavements, an optimal mill-and-inlay depth based on fatigue can be found. Mill-and-inlay strategy may reduce fatigue life of pavements with low traffic volumes. Cost-effectiveness of the mill-and-inlay strategy is higher for pavements with higher traffic. The strategy did not appear to be susceptible to rutting nor did it appear to cause damage to the existing pavement layers.</p>			
<b>16 Key Words</b> Asphalt, Concrete, Pavement, Recycle, Inlay, Milling Depth, Rutting, Transverse Cracking, Falling Weight Deflectometer, Beam, Fatigue, Damage, and Mill-and-Inlay Strategy		<b>17 Distribution Statement</b> No restrictions. This document is available to the public through the National Technical Information Service, Springfield, Virginia 22161	
<b>18 Security Classification (of this report)</b> Unclassified	<b>19 Security Classification (of this page)</b> Unclassified	<b>20 No. of pages</b> 83	<b>21 Price</b>

# **ESTIMATION OF ASPHALT PAVEMENT LIFE**

Final Report

Prepared by

Mustaque Hossain, Ph.D., P.E.  
Associate Professor  
Kansas State University

and

Zhong Wu  
Kansas State University

A Report on Research Sponsored By

THE KANSAS DEPARTMENT OF TRANSPORTATION  
TOPEKA, KANSAS

KANSAS TURNPIKE AUTHORITY  
WICHITA, KANSAS

January 2002

## **PREFACE**

The Kansas Department of Transportation's (KDOT) Kansas Transportation Research and New-Developments (K-TRAN) Research Program funded this research project. It is an ongoing, cooperative and comprehensive research program addressing transportation needs of the state of Kansas utilizing academic and research resources from KDOT, Kansas State University and the University of Kansas. Transportation professionals in KDOT and the universities jointly develop the projects included in the research program.

## **NOTICE**

The authors and the state of Kansas do not endorse products or manufacturers. Trade and manufacturers names appear herein solely because they are considered essential to the object of this report.

This information is available in alternative accessible formats. To obtain an alternative format, contact the Office of Transportation Information, Kansas Department of Transportation, 915 SW Harrison Street, Room 754, Topeka, Kansas 66612-1568 or phone (785) 296-3585 (Voice) (TDD).

## **DISCLAIMER**

The contents of this report reflect the views of the authors who are responsible for the facts and accuracy of the data presented herein. The contents do not necessarily reflect the views or the policies of the state of Kansas. This report does not constitute a standard, specification or regulation.

## **ABSTRACT**

The milling of asphalt concrete (AC) pavement surface refers to the mechanical removal of a part of the pavement surface. The Kansas Department of Transportation (KDOT) and the Kansas Turnpike Authority (KTA) routinely mill the surfaces of some AC pavements before inlaying. KTA has adopted a strategy of recycling the upper pavement layer on a relatively frequent basis (every six or seven years) to maintain a smooth riding surface for the last decade or so. However, in most cases, the milling depth is selected based on the rule-of-thumb or experience of the agency for a specific surface distress, such as rutting or transverse cracking, rather than based on any engineering analysis.

In this report, the structural and functional performances of such mill-and-inlay AC pavements were analyzed for six different routes of KDOT and KTA. All test sections were tested with the Falling Weight Deflectometer (FWD) at 50 to 100 feet intervals before milling, after milling, and after inlaying. Ten 6-inch wide, 18-inch long, full-depth asphalt concrete beams were sawn from four test sections. Fatigue tests were conducted in a third-point flexural loading fashion on those field beams sawn into fatigue test specimens of size: 4-inches wide by 3-inches deep and 16-inches long. Distress models and rational transfer factors were found through the analysis of fatigue test results, deflection data, and historical traffic data to estimate the fatigue damage, functional performance, and rutting susceptibility of the mill-and-inlay pavements. For high traffic pavements, an optimal mill-and-inlay depth based on fatigue can be found. Mill-and-inlay strategy may reduce fatigue life of pavements with low traffic volumes. Cost-effectiveness of the mill-and-inlay strategy is higher for pavements with higher traffic. The strategy did not appear to be susceptible to rutting nor did it appear to cause damage to the existing pavement layers.

## **ACKNOWLEDGMENTS**

The authors wish to acknowledge the financial support for this study provided by the Kansas Turnpike Authority (KTA) and Kansas Department of Transportation (KDOT) under the Kansas Transportation Research and New Developments (K-TRAN) program. Mr. Andrew J. Gisi, P.E., was the project monitor. The authors sincerely thank him for his advice, guidance, and patience during this study.

The authors are indebted to Mr. Don Bruns of Kansas State University, David Jacobson, P.E., Jon Potter, P.E., Tom Wurdeman, P.E. of KTA, Ron Balsters, Mr. Rick Barzenisky, P.E., Paul Barry, P.E., Todd LaTorella, P.E., Mr. Albert Oyerly and the Falling Weight Deflectometer (FWD) crew of KDOT for their zealous cooperation. John Cillessen, P.E., formerly with KTA, provided all field beams from the Kansas Turnpike. His contribution is gratefully acknowledged. Ms. Lea Ann Caffrey, formerly with KDOT, is also thanked for her cooperation in CANSYS data collection. Ms. Linda Pierce of the Washington Department of Transportation provided the EVERCALC software used in this study. Her generosity is gratefully acknowledged.

# TABLE OF CONTENTS

ABSTRACT.....	iv
TABLE OF CONTENTS.....	vi
LIST OF TABLES.....	viii
LIST OF FIGURES .....	ix
CHAPTER 1 .....	1
1.1 Introduction and General Problem Statement.....	1
1.2 Study Objectives.....	2
1.3 Organization of the Report.....	2
CHAPTER 2 .....	4
2.1 Test Sections.....	4
2.2 Traffic History .....	7
2.3 Falling Weight Deflectometer Testing.....	7
2.4 Field Sampling.....	8
2.5 Existing Pavement Condition .....	9
CHAPTER 3 .....	10
3.1 Falling Weight Deflectometer Data Analysis.....	10
3.2 Critical Response Calculation.....	12
CHAPTER 4 .....	14
4.1 Fatigue Tests.....	14
4.2 Fatigue Life Equations.....	14
4.3 Bulk Density and Maximum Theoretical Specific Gravity Tests.....	16
CHAPTER 5 .....	18
5.1 Introduction.....	18
5.2 Estimation of Fatigue Life .....	18
5.3 Fatigue Transfer Functions .....	19
5.4 Effect of Mill-and-Inlay Thickness on Fatigue Life.....	20
5.5 Cost-Effectiveness of Mill-and-Inlay Strategy .....	26
CHAPTER 6 .....	30
6.1 INTRODUCTION .....	30
CHAPTER 7 .....	33
7.1 Introduction.....	33
7.2 Computation of Structural Number .....	33
7.3 Analysis of Serviceability Loss .....	36
7.3.1 AASHTO Equation.....	36
7.3.2 HPMS Equation .....	37

7.4 Comparison of Service and Fatigue Lives .....	40
7.5 Existing Pavement Damage .....	41
CHAPTER 8 .....	47
8.1 Introduction.....	47
8.2 Sensitivity of the Mill-and-Inlay Pavement Thickness Based on Regression Equation...	47
8.3 Determination of the Mill-and-Inlay Thickness from the Equivalent Thickness Method....	50
8.4 Proposed Procedure for Selecting an Optimum Mill-and-Inlay Thickness .....	52
CHAPTER 9 .....	54
9.1 Conclusions.....	54
9.2 Recommendations.....	55
REFERENCES .....	56
APPENDIX A.....	57
APPENDIX B .....	68

## LIST OF TABLES

TABLE 2.1 Test Section Features .....	5
TABLE 2.2 Thickness History of the Test Sections.....	6
TABLE 2.3 Traffic History of the Study Sites .....	7
TABLE 2.4 Existing Pavement Condition.....	8
TABLE 3.1 Backcalculated Layer Moduli (MPa).....	13
TABLE 4.1 Results of the Gmm and Gmb Tests .....	17
TABLE 5.1 Cost-Effectiveness of Mill-and-Inlay Strategies.....	27
TABLE 7.1 Calculated Values of $E_p$ and $SN_{eff}$ of the Test Sections.....	34
TABLE 7.2 Calculated $\Delta$ PSI Values from the AASHTO Equation.....	39
TABLE 7.3 Comparison of $\Delta$ PSI from the AASHTO and HPMS Equations .....	40
TABLE 8.1 Computed Inlay Thicknesses by the Equivalent Thickness Method .....	51

## LIST OF FIGURES

FIGURE 2.1 Test Section Locations .....	6
FIGURE 3.1 Pavement Models Used in Backcalculation Analysis .....	11
FIGURE 3.2 Configuration of A Single Axle and Critical Response Evaluation Points .....	12
FIGURE 5.1 Mill-and-Inlay Thickness vs. Allowable ESALs for I-35, US-59, and K-16 Section (KSU Model) .....	21
FIGURE 5.2 Mill-and-Inlay Thickness vs. Allowable ESALs for I-35, US-59, and K-16 Sections (AI Model) .....	23
FIGURE 5.3 Mill-and-Inlay Thickness vs. Allowable ESALs for Other Test Sections .....	24
FIGURE 5.4 Average Kansas Turnpike Authority Heavy Commercial Truck .....	28
FIGURE 6.1 Mill-and-Inlay Thickness vs. Pavement Service Life (Based on Rutting Depth) ...	32
FIGURE 7.1 Comparison of SN Values .....	35
FIGURE 7.2 Comparison of Serviceability Loss .....	38
FIGURE 7.3 Comparison of Service and Fatigue Lives.....	41
FIGURE 7.4 Horizontal Tensile Strain and Vertical Compressive Strain for I-35 Sections.....	42
FIGURE 7.5 Horizontal Tensile Strain and Vertical Compressive Strain for US-59 Sections....	43
FIGURE 7.6 Horizontal Tensile Strain and Vertical Compressive Strain for K-16 Sections .....	44
FIGURE 7.7 Horizontal Tensile Strain and Vertical Compressive Strain for K-92 Sections .....	45
FIGURE 7.8 Horizontal Tensile Strain and Vertical Compressive Strain for I-335 and K-177 Sections.....	46
FIGURE 8.1 Structural Live vs. Thickness Ratio.....	49

# Chapter 1

## Introduction

### 1.1 Introduction and General Problem Statement

In recent years, the emphasis of highway construction has gradually shifted from new design and construction activities to maintenance and rehabilitation of the existing network. This critical change in highway projects clearly necessitates the development of guidelines for specific major rehabilitation procedures and their engineering consequences. One of these rehabilitation strategies for the asphalt concrete (AC) pavement, mill-and-inlay, has been studied and reported on in this report.

Milling of an asphalt concrete pavement surface refers to the mechanical removal of a part of the pavement surface. There are several applications of the milling process. The most common are (1):

1. Remove an unstable surface that exhibits excessive distresses, such as, roughness, cracking, rutting, or raveling;
2. Increase overhead clearances to provide the required height between the road surface and overhead structures;
3. Reduce pavement build up to eliminate the need to raise guard rails and drainage structure elevations; and
4. Texture the pavement surface to improve skid resistance and provide a smooth riding surface.

The Kansas Department of Transportation (KDOT) and the Kansas Turnpike Authority (KTA) routinely mill the surfaces of some AC pavements before inlaying, which means no

thickness increase happens after rehabilitation. KTA has adopted a strategy of recycling the upper pavement layer on a relatively frequent basis (every six or seven years) to maintain a smooth riding surface for the last decade or so. The assumption is that the existing AC and base layers are in good structural condition to provide extended service lives. However, little is known about the damage of these materials due to this rehabilitation action (mill and inlay) as these layers age and undergo repetitive loading (conducive to fatigue damage) while the top of the surface is being replaced. In most cases, the milling depth is selected based on the rule-of-thumb or experience of the agency for a specific surface distress, such as rutting, rather than basing on any engineering analysis. In fact, no design procedure is available for this rehabilitation since the mill and inlay pavements are not exclusively covered in the 1993 AASHTO Pavement Design Guide (2).

## **1.2 Study Objectives**

The objectives of this research project were:

1. To quantify the structural and functional lives of the mill-and-inlay pavements;
2. To identify damage, if any, of the existing layers of the built-up asphalt pavements on KTA and KDOT network; and
3. To develop a design procedure for the mill-and- inlay pavements.

## **1.3 Organization of the Report**

This report is divided into nine chapters. Chapter 1 is the introduction to the problem. Chapter 2 describes the test sections, traffic history, and data collection. Chapter 3 contains the backcalculation analysis of the pavement layer moduli from the FWD data. Chapter 4 presents the laboratory results of the fatigue tests of asphalt beams. Chapter 5 discusses the prediction of fatigue lives of mill-and-inlay AC pavements based on the analysis of the fatigue test results and

elastic layered pavement systems. Chapter 6 contains the discussion on the rutting potential of the mill-and-inlay pavements. The functional life prediction of the mill-and-inlay pavements is in Chapter 7. Chapter 8 introduces the concept of mill-to-inlay thickness ratio and its effect on pavement fatigue lives. This chapter also presents the recommended procedure for selecting an optimum mill-and-inlay thickness. Finally, Chapter 9 presents the conclusions and recommendations based on this study.

## Chapter 2

### Test Sections, Traffic History, and Data Collection

#### 2.1 Test Sections

Ten 305-meter long AC pavement test sections on six different routes of KDOT and KTA were selected in this project. Table 1 shows the location and general features of these projects. The projects on the I-35 and I-335 are under the jurisdiction of KTA and the rest belong to the KDOT network. All projects are located in the eastern part of the state as shown in Figure 2.1. The majority of the KDOT projects have been built in the 60's and have since been overlaid and seal coated several times leading up to 80's when mill-and-inlaying started. The projects in this study were milled and inlaid during this study period.

The I-35 and I-335 sections were built in late 50's. Since late 80's, these sections have been milled and inlaid at 5- to 8-years intervals. In 1996 and 1997, the existing AC layers of all test sections had been milled to a certain depth before inlaying the same depth with a new AC layer as shown in Table 2.1.

Table 2.2 shows the thickness histories of the test sections. The existing AC thickness indicates the remaining pavement left after milling and inlaying. The I-35, I-335 and K-177 sections have granular bases, the US-59 and K-92 sections are on asphalt bases, and K-16 is a full-depth asphalt pavement built directly on subgrade. The project subgrade soils ranged from ML to CH types.

**TABLE 2.1 Test Section Features**

<b>Route</b>	<b>County</b>	<b>Begin M.P.</b>	<b>End M.P.</b>	<b>Year Built</b>	<b>Last Rehab. Year</b>	<b>Total AC Thickness (mm)</b>	<b>Present Mill- and-Inlay Thickness (mm)</b>
I - 35 S	Sumner	Int.S 23.000 (SB)	23.189	1956	1991	254	64
I - 35 N	Chase	Int.S 102.000 (SB)	102.189	1956	1988	229	50
I-335 N	Osage	Int. S. 156.6 (NB)	156.789	1956	1992	229	50
US-59-1	Anderson	S.C.L 2.000 (SB)	2.189	1962	1988	150	25
US-59-2	Anderson	S.C.L 4.545 (SB)	4.734	1962	1988	150	50
K-16-1	Pottowatomie	W.C.L 5.000 (EB)	5.189	1962	1985	178	38
K-1-2	Pottowatomie	W.C.L 12.000 (EB)	12.189	1965	1988	178	584
K-92-1	Jefferson	W.C.L 6.947 (EB)	7.360	1969	1990	127	25~50
K-92-2	Jefferson	W.C.L 6.947 (WB)	7.360	1969	1990	127	25~50
K-177	Riley	S.C.L 3.000 (SB)	3.189	1953	1992	267	150

*Note: Int. S - Interstate Highway System; W.C.L - West County Line; and S.C.L - South County Line.*



**FIGURE 2.1 Test Section Locations**

**TABLE 2.2 Thickness History of the Test Sections**

<b>Route</b>	<b>AC Inlay Thickness (mm)</b>	<b>Remaining AC Thickness (mm)</b>	<b>Base Thickness (mm)</b>	<b>Subgrade Soil Type</b>
<b>I-35 S</b>	64	191	457	CL, ML
<b>I-35 N</b>	50	178	457	ML-CL, or CH
<b>I-335</b>	50	178	457	ML-CL, or CH
<b>U-59-1</b>	25	127	150	ML, CL or CH, CL
<b>U-59-2</b>	50	102	150	ML, CL or CH, CL
<b>K-16-1</b>	50	150	---	CL, CH, ML or MH
<b>K-16-2</b>	50	140	---	CL, CH, ML or MH
<b>K-92-1</b>	50	89	203	CL, ML, CH
<b>K-92-2</b>	25	114	203	CL, ML, CH
<b>K-177</b>	150	114	229	CL, CH, or ML

**TABLE 2.3 Traffic History of the Study Sites**

<b>Route</b>	<b>1996 ADT</b>	<b>% Commercial</b>	<b>Current Annual ESAL=s (on design lane)</b>	<b>Cumulative ESAL's since last Rehabilitation</b>
<b>I - 35 S</b>	15,120	13	388,816	1,881,875
<b>I - 35 N</b>	10,443	13	268,841	1,901,376
<b>I-335</b>	2,796	13	146,000	1,405,070
<b>US-59-1</b>	1,180	15	12,775	163,515
<b>US-59-2</b>	1,120	16	22,630	166,085
<b>K-16-1</b>	665	8	4,380	17,928
<b>K-16-2</b>	710	6	4,380	35,797
<b>K-92-1</b>	1,870	5	6,205	24,696
<b>K-92-2</b>	1,870	5	6,205	24,696
<b>K-177</b>	5,885	6	39,055	173,832

## **2.2 Traffic History**

Table 2.3 shows the 1996 AADT and past traffic histories of the sections. For the given test sections, historical traffic data was collected from 1988 to 1997 and translated into annual 18-kip Equivalent Single Axle Load (ESAL) values to compute cumulative ESAL values since last rehabilitation. The I-35 sections had higher traffic loads than the other sections.

## **2.3 Falling Weight Deflectometer Testing**

The pavement test sections were tested with a Falling Weight Deflectometer (FWD) at 15.25 to 30.5-meter intervals before milling, after milling, and after inlay. The target load levels were 40 kN and 67 kN. At each test station, four drops of the FWD load (two around 40 kN and the other

two around 67 kN) were used. Seven sensors were used at a uniform spacing of 300 mm. The air and pavement surface temperatures during test period were automatically recorded.

## 2.4 Field Sampling

Ten 150 mm (6 in.) wide, 457 mm (18 in.) long, full-depth asphalt concrete beams were sawn from each of the test sections on I-35, US-59 and K-16 at approximately 30 meter intervals after mill-and-inlay. Almost all beams on the I-35 North project were intact. Delamination and cracking of the existing asphalt layers were evident on some of the beams from the I-35 South site. Overall, I-35 North beams were found to be in excellent condition. The beams from US-59 and K-16 were also in good condition. Some photographs showing these beams are attached to the Appendix A.

**TABLE 2.4 Existing Pavement Condition**

Route	County	Longitudinal/ Fatigue Cracking	Rutting (6 mm - 12.5 mm)	Trans- verse Cracking	Avg. Wheelpath IRI (before Mill & Inlay) (m/km)	PSI*
I - 35 S	Sumner	✓	✓	✓	1.72	3.12
I - 35 N	Chase	✓	✓	✓	1.51	3.24
I-335	Osage	✓	✓	✓	1.67	3.32
US-59-1	Anderson	✓	✓	✓	1.67	3.14
US-59-2	Anderson	✓	✓	✓	1.81	3.30
K-16-1	Pottowatomie		✓	✓	1.85	2.89
K-16-2	Pottowatomie		✓	✓	1.77	3.16
K-92-1	Jefferson	✓	✓	✓	1.77	3.03
K-92-2	Jefferson	✓	✓	✓	1.77	3.03
K-177	Riley		✓	✓	1.15	3.72

\* based on the FHWA HMPS Equation

## **2.5 Existing Pavement Condition**

Most of the sites were visited before rehabilitation and quantitative distress information was obtained from the KDOT's pavement management system database. Table 2.4 shows a checklist of distresses found on each site. The most common distresses found were longitudinal or fatigue cracking, transverse cracking, and rutting. Severe fatigue cracking was observed on US-59 and K-92 sites, while some other sites had only longitudinal cracking. On the average, each site had about 6.5 mm to 12.5 mm rutting. Rut depths on several stations were higher than 12.5 mm. Transverse cracking was observed on all sites. These distresses contributed to the roughness shown in the last column of Table 4. Only K-177 had lower severity of all distresses mentioned, and that is well reflected in its lower International Roughness Index (IRI) value than other sites.

## Chapter 3

### Backcalculation of Pavement Layer Moduli and Computation of Critical Responses

#### 3.1 Falling Weight Deflectometer Data Analysis

As mentioned earlier, three different sets of FWD data were collected on each test section—before milling, after milling, and after inlay. FWD data was collected at 11 stations (or 21 stations), at 30.5 meters (or 15.25 meter) intervals, on a 305-meter long test section. A linear elastic backcalculation program EVERCALC, developed by the Washington Department of Transportation, was used to analyze the deflection data. The pavements were modeled as a four-layer structure (before milling and after milling) and a five-layer structure (after inlay), as shown in Figure 3.1. The backcalculation results were based on the FWD deflections corresponding to a 40 kN target load. The root-mean-square (RMS) values were generally kept below 2 percent, and the basins, which had higher RMS values, were discarded. The backcalculated moduli of the AC layer corresponded to the temperatures at which deflection testing was conducted, and were later adjusted to a pavement temperature of 20° C. The equation used to perform the temperature adjustments was developed by Braun Intertec based on the LTPP data (3):

$$\frac{E_1}{E_2} = 10^{0.01*(T_2 - T_1)} \quad (\text{Equation 3-1})$$

where:  $E_1$  = Modulus at temperature  $T_1$  °F; and

$E_2$  = Modulus at temperature  $T_2$  °F.

4-Layer Structure	5-Layer Structure
Existing AC	AC Inlay Layer
	Existing AC
Base Layer	Base Layer
Subgrade	Subgrade
Stiff Layer	Stiff Layer

**FIGURE 3.1 Pavement Models Used in Backcalculation Analysis**

A model developed by Witczak (4) was used to estimate the pavement temperature at mid-depth of the AC layer:

$$MMPT = MMAT * \left[ 1 + \frac{1}{z + 4} \right] - \frac{34}{Z + 4} + 6 \quad (\text{Equation 3-2})$$

where: MMPT = Mean monthly AC pavement temperature at depth Z.

MMAT = Mean monthly air temperature.

After adjustments to 20 °C, modulus values greater than the practical limits (8610 MPa) were excluded from the analysis. The spatial variation of the pavement layer moduli was determined by averaging the values at all test points within the section being analyzed. For computing critical pavement responses to traffic loading, the mean values of the existing pavement layer moduli were taken corresponding to FWD data before milling, after milling, and after inlay as tabulated in Table 3.1. The table shows that the coefficients of variation of the AC

moduli were fairly similar for the existing AC and inlay layers. In general, the backcalculation results were judged to be good.

### 3.2 Critical Response Calculation

The layered elastic analysis program, ELSYM5, was used to find the critical tensile strain at the bottom of the existing AC layer at three points in the pavement structure subjected to a standard 80 kN (18-kip) dual wheel load with 690 kPa (100 psi) tire pressure. The points, 1, 2 and 3, as shown in Figure 3 correspond to the center of the left wheel, the right edge of the left wheel and in-between the wheels, respectively. The backcalculated elastic moduli of the pavement layers were used to characterize the layers. The highest of these three tensile strain values was taken as the critical tensile strain at the bottom of the existing AC layer and used in the pavement fatigue life analysis discussed later.

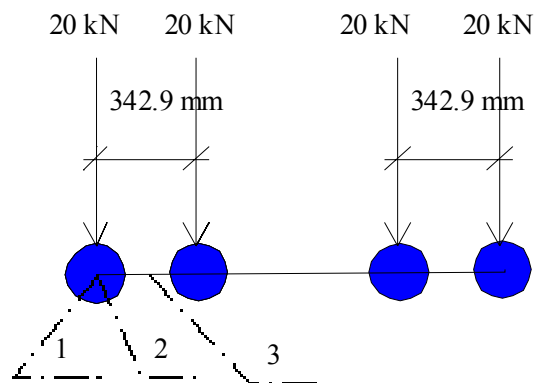


**FIGURE 3.2 Configuration of A Single Axle and Critical Response Evaluation Points**

**TABLE 3.1 Backcalculated Layer Moduli (MPa)**

Site	Statistic	AC Inlay	Existing AC	Asphalt Treated Base	Granular Base	Subgrade
<b>I-35 S</b>	mean	1550	1468	-	172	138
	s	703	565	-	48	48
	cov (%)	276	269	-	193	234
	n	83	158	-	152	158
<b>I-35 N</b>	mean	4899	3479	-	241	138
	s	2122	1640	-	34	41
	cov (%)	289	324	-	96	207
	n	55	103	-	103	103
<b>I-335</b>	mean	4272	1468	-	138	96
	s	262	427	-	41	34
	cov (%)	41	200	-	207	248
	n	69	103	-	124	124
<b>US-59-1</b>	mean	4623	5257	1116	-	69
	s	1936	2281	441	-	14
	cov (%)	289	296	276	-	152
	n	69	110	110	-	110
<b>US-59-2</b>	mean	6442	5987	1282	-	62
	s	2914	2163	593	-	14
	cov (%)	310	248	317	-	138
	n	41	90	90	-	90
<b>K-16-1</b>	mean	3176	5650	-	-	48
	s	758	2005	-	-	14
	cov (%)	165.36	241	-	-	158
	n	41	83	-	-	103
<b>K-16-2</b>	mean	6270	8075	-	-	76
	s	1454	2150	-	-	21
	cov (%)	158	186	-	-	193
	n	41	55	-	-	117
<b>K-92-1</b>	mean	1833	3989	613	-	76
	s	903	1812	296	-	21
	cov (%)	338	310	338	-	193
	n	69	69	83	-	117
<b>K-92-2</b>	mean	4706	4368	607	-	62
	s	1647	2308	207	-	14
	cov (%)	241	365	234	-	138
	n	55	76	90	-	90
<b>K-177</b>	mean	5581	2660	-	351	117
	s	1226	1509	-	186	41
	cov (%)	152	393	-	358	241
	n	55	124	-	124	124

## Chapter 4

### Laboratory Tests

#### 4.1 Fatigue Tests

The field beams retrieved from the sites on I-35 S, I-35 N, US-59, and K-16 were sawn into fatigue test specimens of size 101.6 mm wide, 76.2 mm deep and 406.4 mm long at Kansas State University. Two sets of samples were prepared - the first set incorporating the newly-built inlay layer, and the second set consisting solely of the existing asphalt layer. Fatigue tests were done in a third-point flexural loading fashion using a sinusoidal load of 10 Hz frequency. Constant stress mode was chosen in the flexural tests and the test temperature was controlled at 20 °C. The initial tensile strain was measured at the bottom fiber of the beams at the 200th repetition of the applied load, and then the beams were loaded to failure. The applied load was varied so that a range of tensile strains and corresponding varied failure cycles would be obtained.

#### 4.2 Fatigue Life Equations

The stiffness modulus and the initial strain of the asphalt beam during each test were determined at the 200th repetition by using Equations 4-1 and 4-2, respectively (5).

$$E_s = \frac{P_A(3L^2 4a^2)}{4bh^3\Delta} \quad (\text{Equation 4-1})$$

$$\varepsilon_t = \frac{\sigma}{E_s} = \frac{12h\Delta}{3L^2 4a^2} \quad (\text{Equation 4-2})$$

where:  $E_s$  = flexural stiffness modulus;

$\varepsilon_t$  = Initial tensile strain;

P = total dynamic load;

h = specimen height;

b = specimen width;

L = beam span length;

a = distance between support and the first applied load; and

$\Delta$  = beam center deflection.

A relationship was established for the initial strain,  $\varepsilon$ , versus the fatigue life,  $N_f$  for each test section from a least-square regression analysis, and can be shown (in generic form) as: (5)

$$N_f = K_2 (1/\varepsilon)^{n_2} \quad (\text{Equation 4-3})$$

where

$N_f$  = number of load applications to failure;

$K_2$  = constant depending on the mix;

$\varepsilon$  = initial bending strain based on center point deflection of specimen; and

$n_2$  = constant (slope of regression line).

The following power regression equations of fatigue lives were obtained for the asphalt mixtures at 20° C on different sections:

Interstate-35 South (I-35S):

$$\ln(N_f) = 24.4478 - 3.0795 \ln(\varepsilon_r) - 3.344 \ln(E_{AC}) \quad (R^2 = 0.721) \quad (\text{Equation 4-4})$$

Interstate-35 North (I-35N):

$$\ln(N_f) = 20.7502 - 4.2438 \ln(\varepsilon_r) - 3.5175 \ln(E_{AC}) \quad (R^2 = 0.818) \quad (\text{Equation 4-5})$$

US Highway 59 (US-59-1):

$$\ln(Nf) = 10.0185 - 1.932\ln(\varepsilon_r) - 1.222\ln(E_{AC10}) \quad (R^2 = 0.798) \quad (\text{Equation 4-6})$$

Kansas Highway 16 (K-16-1):

$$\ln(Nf) = 48.356 - 0.143\ln(\varepsilon_r) - 3.309\ln(E_{AC10}) \quad (R^2 = 0.719) \quad (\text{Equation 4-7})$$

The  $R^2$  values for all sections were very satisfactory considering the fact that the lower layer materials were very old and may be nonhomogeneous.

### **4.3 Bulk Density (Gmb) and Maximum Theoretical Specific Gravity (Rice) (Gmm) Tests**

These tests were done according to the applicable ASTM procedures on the samples taken from the field beams. For bulk density, samples were sawn out of the outer third of the broken beams in the fatigue tests. The loose samples for the “Rice” tests were obtained by heating the broken beam samples. Test results are shown in Table 4.1 along with the computed air voids. The air void was found from the Gmm and Gmb values, using the following equation:

$$\text{Air Void(\%)} = 100 - (\text{Gmb/Gmm}) * 100 \quad (\text{Equation 4-8})$$

**TABLE 4.1 Results of the Gmm and Gmb Tests**

<b>Route</b>	<b>Beam ID</b>	<b>Gmm</b>	<b>Gmb</b>	<b>Air Void (%)</b>
<b>I-35 S</b>	100-Bottom	2.448	2.273	7.15
	100-Top	2.429	2.289	5.76
	500-Bottom	2.45	2.249	8.20
	500-Top	2.44	2.293	6.02
<b>I-35 N</b>	100-Bottom	2.43	2.35	3.29
	100-Top	2.475	2.361	4.61
	500-Bottom	2.465	2.358	4.14
	500-Top	2.438	2.337	4.34
<b>US-59-1</b>	100-Bottom	2.452	2.211	9.83
	100-Top	2.445	2.34	9.02
	500-Bottom	2.452	2.23	4.30
	500-Top	2.455	2.321	5.09
<b>US-59-2</b>	100-Bottom	2.446	2.272	7.12
	100-Top	2.457	2.386	2.91
	500-Bottom	2.446	2.294	6.23
	500-Top	2.457	2.359	3.99
<b>K-16-2</b>	100-Bottom	2.411	2.316	3.93
	100-Top	2.397	2.253	6.02
	500-Bottom	2.411	2.222	7.81
	500-Top	2.397	2.249	6.15

## Chapter 5

### Fatigue Life Prediction

#### 5.1 Introduction

It is well known that the asphalt layer modulus increases with pavement age. Some researchers think that such an increase in AC modulus will enhance its load-spreading ability, and will result in a reduction of traffic-induced tensile strain at the bottom of the AC layer which is generally known to be responsible for fatigue of the AC layer (6, 7). Table 3.1 shows that on US-59, K-16, K-92, and K-177, in general, the existing AC moduli were either higher than or closer to the inlay AC moduli. However, the opposite is true for I-35. The traffic histories in Table 2.3 show that the sections on I-35 carried significantly higher traffic (ESAL's) than the other sections. Due to traffic loading, the existing AC layers on I-35 sections were severely cracked and in some places, delaminated (some field beams showed this evidence). Therefore, it is apparent that the traffic history on the AC pavement plays an important role in its material property determination as well as in degradation.

#### 5.2 Estimation of Fatigue Life

The fatigue lives were estimated using the Equations 4-4 to 4-7. The elastic modulus used in the fatigue model is the weighted AC modulus for the pavement. It represents the overall modulus of the AC inlay and existing AC layers, and was calculated by:

$$E_{AC} = (E_1 \times h_1 + E_2 \times h_2) / (h_1 + h_2) \quad (\text{Equation 5-1})$$

where:  $E_1$ ,  $h_1$  stands for the modulus and thickness of the AC inlay layer, respectively, and

$E_2$ ,  $h_2$  stands for the modulus and thickness of the existing AC layer, respectively.

This modulus was selected because the laboratory fatigue life prediction models were based on the fatigue test results from both new and existing pavement beams. This approach is correct since in the mill-and-inlaid pavement, both new and existing layers are expected to resist fatigue cracking in a composite manner.

### **5.3 Fatigue Transfer Functions**

Fatigue transfer functions relate the allowable number of ESAL's before a certain extent of fatigue cracking to the strain (horizontal tensile strain at the bottom of the AC layer) caused by an 80 kN (18-kip) single axle load. The laboratory fatigue model may be used to predict the actual number of ESAL's on the pavements in the field after multiplication with this transfer factor.

According to the rehabilitation history record, the I-35, US-59 and K-16 projects had been rehabilitated by the mill-and-inlay procedure about 6 to 8 years ago. The mill-and-inlay thicknesses and the traffic (ESAL's) carried from the last rehabilitation to the current one are shown in Tables 2 and 3, respectively. The rehabilitation need could result from the pavement distresses observed- fatigue cracking, transverse cracking, high rut depths, etc. Those distresses, in turn, translate into intolerable roughness. Condition histories show that all test sections on I-35, US-59 and K-16 had all of these distresses, and resulted in mill-and-inlay action in the recent past. Since the past traffic (ESAL's) is known, it is reasonable to assume that the fatigue transfer factor can be calculated for each test section by dividing the past traffic (ESAL's) by the fatigue cycles to failure derived from the laboratory fatigue models using both new and existing asphalt beam samples. The allowable ESAL's computed by the fatigue models may be interpreted as the composite fatigue life of a certain mill-and-inlay AC pavement. The transfer factors for the four sections for which laboratory fatigue tests were available are:

I-35 S,         $f = 4.33$ ;                      I-35 N,         $f = 1.81$ ;  
US-59-1,       $f = 1.46$ ;                      K-16-2,       $f = 618.7$ ;

The transfer factors varied widely due to the different mixes used on these projects over the years. For the K-16-2 project, the factor is unusually high. This may indicate that the fatigue test results on these projects are not “transferable” probably due to lower traffic repetitions, and the “life” of the pavement since the last rehabilitation has not been consumed by fatigue. This was confirmed by the absence of any longitudinal/fatigue cracking on this project (Table 2.4).

#### **5.4 Effect of Mill-and-Inlay Thickness on Fatigue Life**

Figure 5.1 shows the relationship between the mill-and-inlay thickness versus the allowable ESAL’s for I-35, US-59-1 and K-16-1. The figure shows that on I-35, with an increase in mill-and-inlay thickness, the allowable ESAL’s first increases to a maximum value, then decreases. For the I-35 South section, it appears that the allowable ESAL’s to fatigue failure do not vary much for 25 to 75 mm of milling thickness. However, for the I-35 North section, the same thickness range would be from 25 to 50 mm. This means that the milling thickness has a critical range of values on I-35, outside which, the fatigue life will decrease.

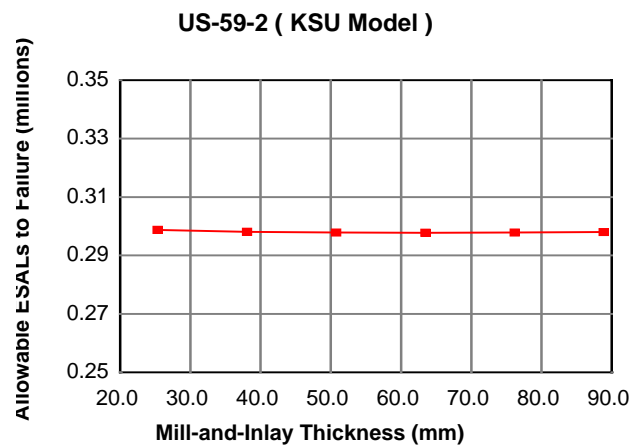
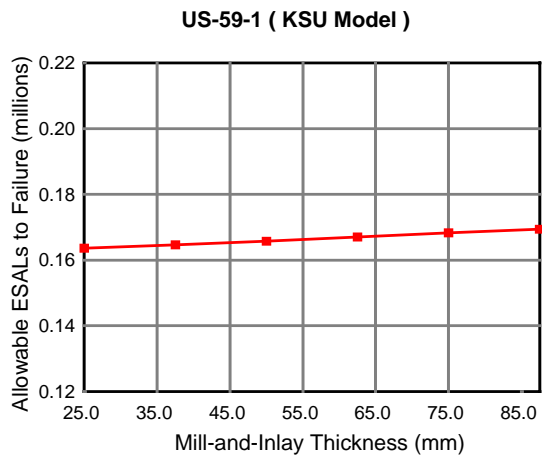
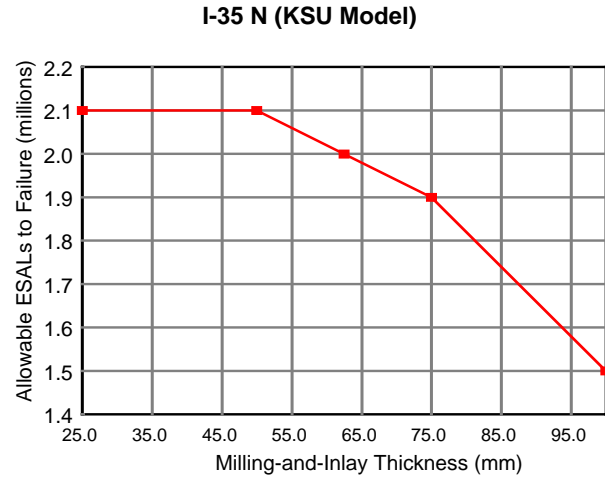
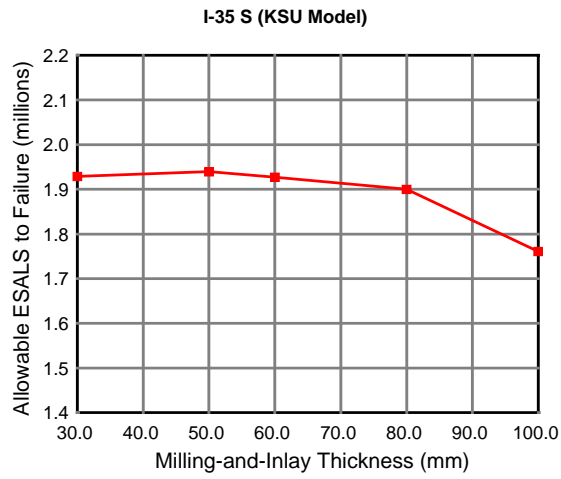


**FIGURE 5.1 Mill and Inlay Thickness vs. Allowable ESALs for I-35, US-59, and K-16 Sections (KSU Model)**

In order to verify this observation, the Asphalt Institute (AI) fatigue model was used. The AI fatigue model can be expressed as:

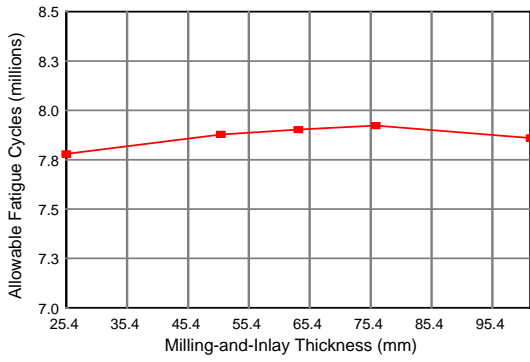
$$N_f = 0.0796 * (\varepsilon_t)^{-3.291} * (E_{AC})^{-0.854} \quad \text{(Equation 5-2)}$$

where:  $N_f$  = Number of load repetitions to failure;  
 $\varepsilon_t$  = Tensile strain at the bottom of the AC layer; and  
 $E_{AC}$  = Modulus of the AC layer.

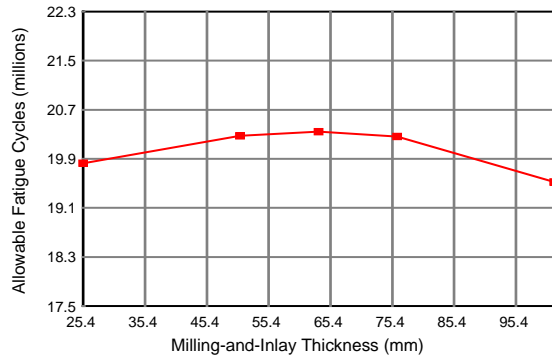
Figure 5.2 shows that the mill-and-inlay thickness versus the allowable ESAL's curve using the AI fatigue model. It is apparent that both Figures 5.1 and 5.2 show similar trend. However, the critical mill depth range for the AI model is 50 to 75 mm for both I-35 South and North sections. Comparing these two sections, it is apparent that the milling depth on these I-35 sections should be between 50 to 75-mm. This observation is confirmed by Figure 5.3, which shows the mill-and-inlay thickness versus allowable fatigue cycles (millions) to failure relationship for I-335. The optimum mill-and-inlay thickness range is also from 50.8 to 76.2 mm for I-335.

The other factor, which needs to be considered in the mill depth selection process is the reflection cracking due to transverse cracks on the existing pavement. With the rule-of-thumb of 25.4-mm crack propagation per year, a 50.8 mm milling depth should give a two-year window before any reflection cracking happens. However, even after cracking, if the cracks could be maintained in an effective manner with local maintenance, the pavements could be operated in a satisfactory serviceable (roughness) condition, provided no fatigue-related cracking or rutting occurs. This is only possible by providing a fatigue-resistant inlay of rut-resistant asphalt mixture.

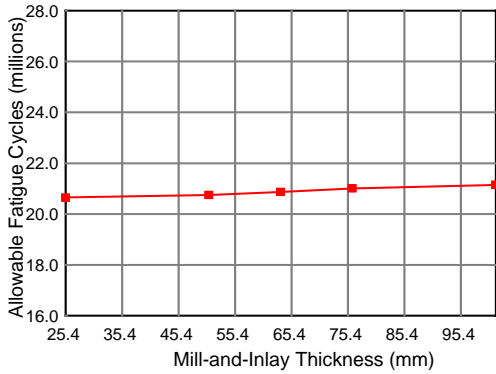
I-35 S (AI Model)



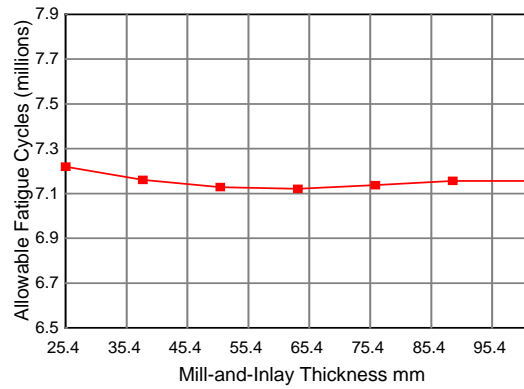
I-35 N (AI Model)



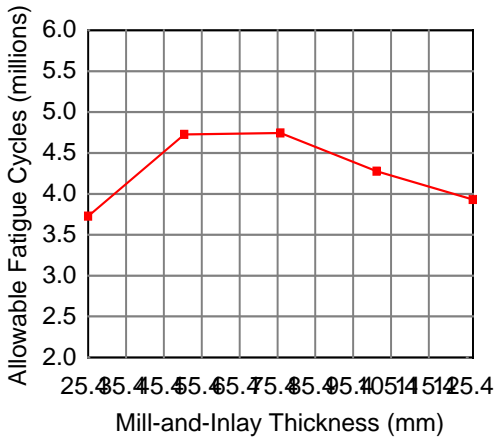
US-59-1 (AI Model)



K-16-2 (AI Model)



I-335 (AI Model)



US-59-2 (AI Model)

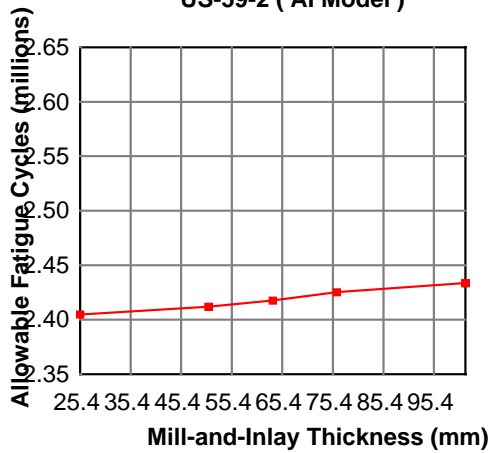


**FIGURE 5.2 Mill-and-Inlay Thickness vs. Allowable ESALs for I-35, US-59, and K-16 Sections (AI Model)**

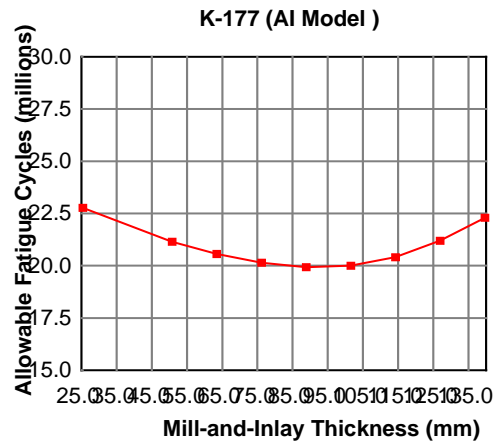
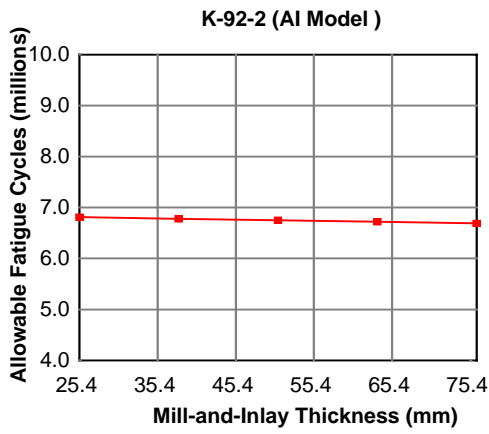
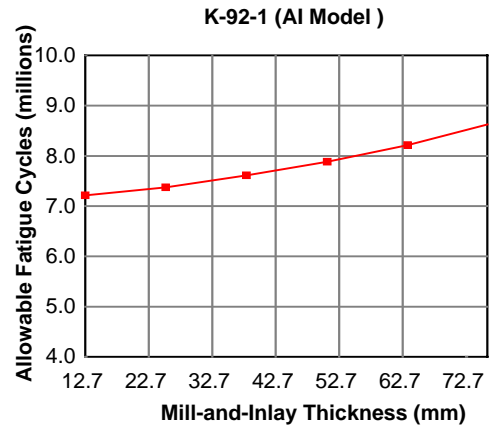
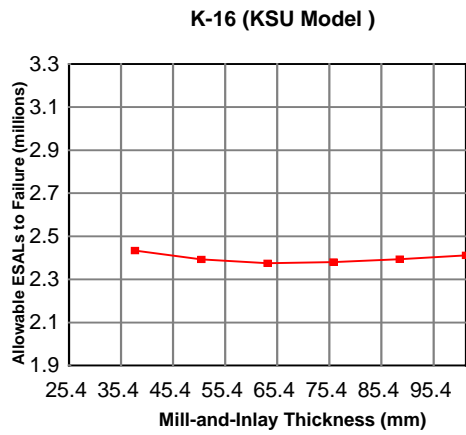


**FIGURE 5.3 Mill-and-Inlay Thickness vs. Allowable ESALs for Other Test Sections (AI Model)**

On US-59-1, the curve of allowable ESAL's versus mill-and-inlay thickness, as shown in Figure 5.1, is much flatter. Both KSU and AI models show that the mill-and-inlay thickness would steadily increase in allowable fatigue life. However, the difference is not significant for milling depths of 37 to 64 mm. The AI model shows that on US-59-2, the fatigue life would slowly increase with an increase in mill-and-inlay thickness and then decrease. Here again, the difference is insignificant for the mill-and-inlay thickness of 38.1 to 76.2 mm. This insensitivity of the fatigue life toward the mill-and-inlay depth could be attributed to two facts: (i) the inlay and the existing pavement moduli on this project are close, and (ii) an asphalt base is present. This phenomenon is also evident on K-92-2 where an asphalt base layer also is present (Figure 5.3). The fatigue life of K-92-1, which has a lower inlay modulus than the existing pavement, is slightly more sensitive to the mill-and-inlay depth.

Figures 5.1 and 5.3 also show that the fatigue lives of both K-16 sites would decrease with an increase in mill depth up to 50 mm and then would remain relatively constant. This apparently happens due to very high moduli of the existing AC layers. No evidence of fatigue cracking was found on the K-16 sections. The sections were rehabilitated for severe transverse cracking. Observed on this section just before rehabilitation in 1997, were 48 full-width transverse cracks with noticeable roughness per mile.

Figure 5.3 also shows the fatigue life versus mill-and-inlay thickness relationship for K-177. This section is unique in a sense that the milling was quite deep on this section, 150 mm. The section was also rehabilitated because of severe transverse cracking although no fatigue crack was found. Figure 5.2 shows that the fatigue life would decrease with an increase in mill depth up to 100-mm and then would increase. Results from K-16 and K-177 tend to indicate that

if the fatigue-related distresses are not present on a section, mill-and-inlay strategy may result in a loss of fatigue life.

### 5.5 Cost-Effectiveness of Mill-and-Inlay Strategy

The cost-effectiveness of mill-and-inlay strategy is of very much interest to both KDOT and KTA. Current costs associated with the mill-and-inlay strategy for a 4-lane mile, 7.47-meter wide project of KDOT and KTA are given below:

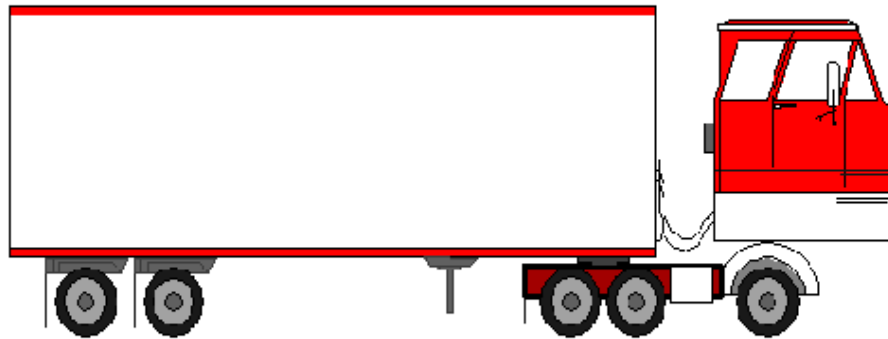
AGENCY	MILL AND INLAY THICKNESS (mm)	COST (\$)
KDOT	25	72,000
	50	108,000
	64	180,000
	76	216,000
KTA	25	70,000
	50	101,000
	64	145,000
	76	173,000

A cost comparison of different mill-and-inlay thicknesses for a 6.2 m wide, 2-lane 1.61 km project on I-35 and a 2-lane 1.61 km project on US-59 is shown in Table 5.1. It is apparent that 25-mm mill-and-inlay thickness is the least-cost strategy for both sections on I-35. The cost disproportionately increases for a mill-and-inlay thickness greater than 50 mm. Experience has shown that a 25-mm inlay deteriorates (increases in roughness) at a faster rate than a 50 mm inlay. Thus, a 50-mm inlay appears to be the most cost-effective strategy for the pavements on I-35 for KTA. However, this strategy needs to be applied at a regular intervals, such as approximately 4 years for the south section and about 6 years for the north section, or, on an average of 5-year intervals.

**TABLE 5.1 Cost-Effectiveness of Mill-and-Inlay Strategies**

<b>Pavement</b>	<b>Mill-and-Inlay Thickness (mm)</b>	<b>ESAL Capacity (x 1,000)</b>	<b>Life (years)</b>	<b>Total Cost (\$)</b>	<b>Unit Cost (\$/ESAL-mile)</b>
<b>I-35 S</b>	25.4	1,924.4	4.21	38,588	0.020
	50.8	1,940.0	4.23	48,500	0.025
	63.5	1,927.9	4.21	73,260	0.038
	76.2	1,900.1	4.16	85,505	0.045
<b>I-35 N</b>	25.4	2,066.0	6.31	30,990	0.015
	50.8	2,083.3	6.35	52,083	0.025
	63.5	2,028.1	6.21	70,984	0.035
	76.2	1,913.3	5.90	86,099	0.045
<b>US-59</b>	25.4	165.1	10.24	35,981	0.22
	38.1	166.8	10.34	53,971	0.32
	50.8	168.6	10.45	71,962	0.43
	63.5	170.6	10.56	89,952	0.53
	76.2	172.6	10.68	107,942	0.63

**SN = 5,  $P_t = 2.5$**



$$\begin{array}{r} 151 \text{ kN} \\ 34,000 \text{ lb} \\ 1.10 \end{array} + \begin{array}{r} 151 \text{ kN} \\ 34,000 \text{ lb} \\ 1.10 \end{array} + \begin{array}{r} 54 \text{ kN} \\ 12,000 \text{ lb} \\ 0.19 \end{array} = 2.39 \text{ ESALs}$$

**FIGURE 5.4 Average Kansas Turnpike Authority Heavy Commercial Truck**

In 1997, the average toll on KTA for the commercial vehicle was \$6.29 for an average 60-mile trip or about 10.5 cents per mile. Assuming the average commercial vehicle on KTA has an ESAL value of 2.39, as shown in Figure 5.4, the average toll translates to 4.4 cents per ESAL-mile ( $\$0.105/2.39$ ). Thus, for a typical 50-mm inlay on I-35, the pavement construction cost would represent about 57 percent of the toll being collected now. The 1982 Final Report on the Federal Highway Cost Allocation Study calculated efficient pavement damage charges by functional system ranging from 8.7 cents per ESAL mile on rural Interstates to 69.1 cents per mile on urban Interstates (8). However, in 1994, Hutchinson and Haas estimated that the marginal pavement damage costs for a pavement with 500,000 annual ESAL's as 3.3 cents per ESAL-mile (9).

Table 5.1 shows that a 25-mm inlay on US-59 would cost about 22 cents per ESAL-mile and would last about 10 years. However, a 50-mm inlay would not add any more life to the pavement but would cost almost double (43 cents versus 22 cents for 25.4 mm). Assuming that the I-35 South project would be inlaid two times in 10 years, the cost of a 50 mm inlay is 5 cents per ESAL-mile (in 10 years) for I-35 as compared to 43 cents per ESAL-mile for US-59. That is eight times more expensive! However, this is not surprising. Deacon developed a model using the AASHTO pavement design and performance equations to estimate the changes in pavement rehabilitation costs resulting from increases or decreases in pavement loadings (10). His results showed that when viewed in terms of cents per ESAL mile, pavement costs are much higher on low traffic roads than on high traffic roads. Hutchinson and Hass have also shown that cost per ESAL on highways designed for 500,000 ESAL's per year is almost four times as great as the cost per ESAL on highways designed for 2,000,000 ESAL's per year (9).

## Chapter 6

### Rutting Susceptibility of the Mill-and-Inlay Strategy

#### 6.1 Introduction

Rutting is an important factor in flexible pavement performance. With the increase in traffic load and tire pressure, most of the permanent deformation now occurs in the upper layers of pavements than in the subgrade. The AASHTO road test results showed that about 91 percent of the rutting occurred within the pavement itself, with 32 percent in the surface, 14 percent in the base, and 45 percent in the subbase (5). Thus, only 9 percent of a surface rut could be accounted for by rutting of the subgrade. Data also showed changes in the thickness of the component layers were not caused by the increase in density but due primarily to lateral movements of the materials. Other studies also showed that in the asphalt layer in only top one-third of total AC thickness would contribute to more than 50 percent rutting caused in this layer (11). This indicates that the mill-and-inlay layer would be more susceptible to rutting than any other layers in the rehabilitated pavements.

Generally, there are two approaches in the design methods which have been used to control rutting: one to limit the vertical compressive strain on the top of subgrade, and the other to limit the surface rutting to a tolerable amount, say 12.5 mm. Since rutting is due primarily to the decrease in thickness of the component layers above subgrade, as was found in the AASHTO Road Test and in research by others, use of the second method should be more appropriate. Ali and Tayabji developed the following equation using the Long- Term Pavement Performance (LTPP) data (7):

$$\rho_p = 0.00011 h_{AC} \left[ \sum_{i=1}^k n_i (\epsilon_{AC})^{\frac{1}{1.111}} \right]^{0.9} + 23.36 h_{Base} \left[ \sum_{i=1}^k n_i (\epsilon_{Base})^{20} \right]^{0.05} + 0.022 h_{Subgrade} \left[ \sum_{i=1}^k n_i (\epsilon_{Subgrade})^{2.81} \right]^{0.356}$$

- where:  $\rho_p$  = Cumulative permanent deformation (rutting) in all layers;;
- $n_i$  = Number of applications of load group  $i$ ;
- $\epsilon_{AC}$ ,  $\epsilon_{Base}$ ,  $\epsilon_{Subgrade}$  = Vertical compressive strain in the middle of layers of AC, base and subgrade (generally the subgrade is divided into several sublayers until the vertical compressive strain is close to zero); and
- $h_{AC}$ ,  $h_{Base}$ ,  $h_{Subgrade}$  = Thickness of AC, base, and sublayers of subgrade, respectively.

The advantage of above model may lie in that it is particularly suitable for investigating the sensitivity of rutting to traffic load, pavement design and material properties. However, the equation may not be applicable universally since the parameters are from the regression analysis. In this research, the rutting potential of the existing and mill-and-inlay pavements was studied using this equation. The past traffic (ESAL's) since the last rehabilitation was assumed to have caused 12.5-mm of rutting on the existing AC pavements. The actual rutting was 6 to 12.5 mm. The mill-and-inlay depth versus the calculated service life (*defined as the time period in years to allowable rut depth of 12.5 mm on the mill-and-inlay AC pavements*) relationships are shown in Figure 6.1. The figure shows that the service life of the mill-and-inlay AC pavement based on rutting is fairly insensitive to the mill-and-inlay thickness. This implies that there is no significant change of rutting potential for the mill-and-inlay AC pavements no matter what mill-and-inlay thickness is selected. Since the mill-and-inlay thickness is usually relatively small compared to the total AC thickness, and the overall pavement structure is

not being changed, the rutting potential of this type of pavements can be considered insignificant. However, this analysis assumes that the mixture and construction process would not contribute to the rutting on the inlays, and thus, the inlay mixture should not have any rutting potential

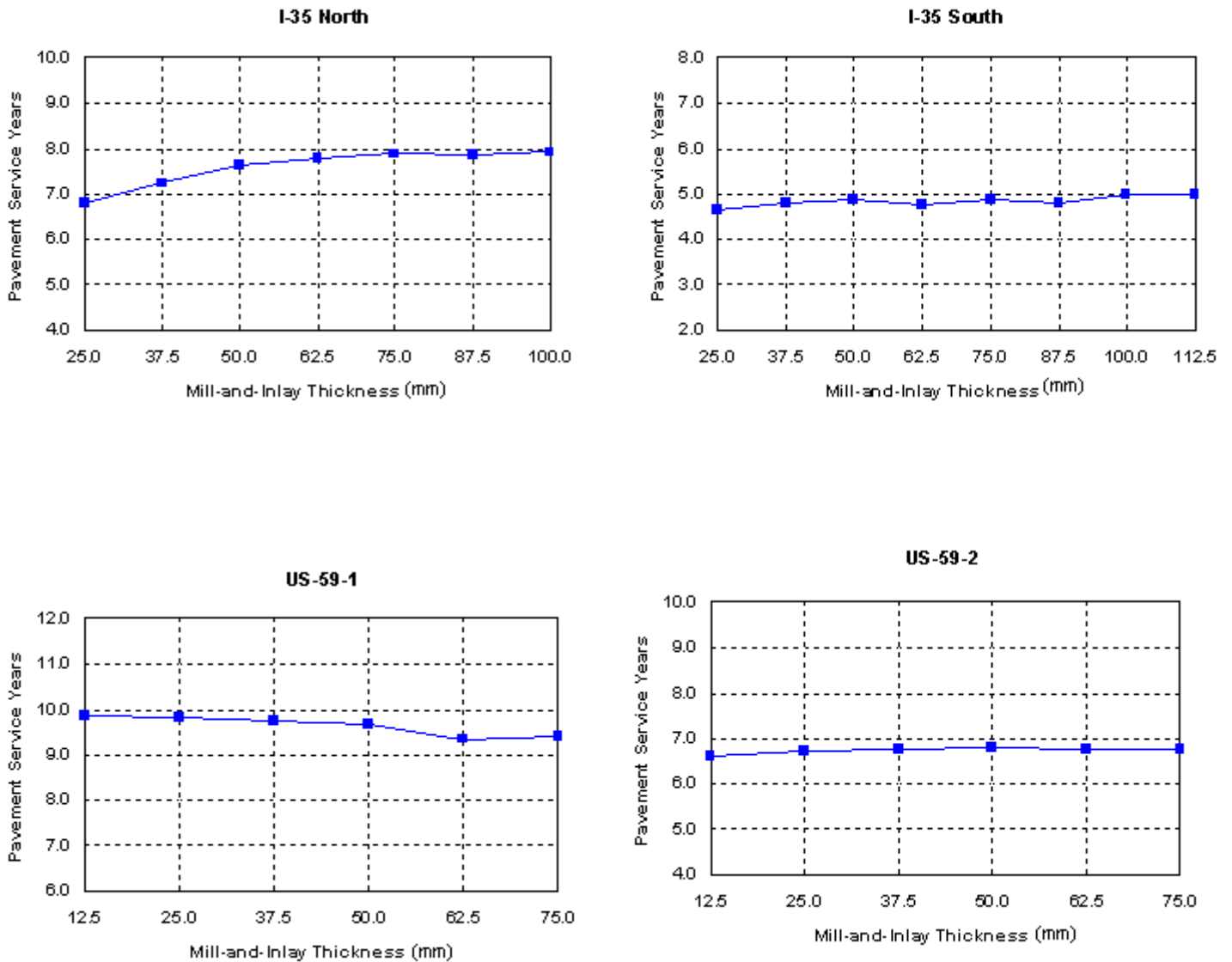


**FIGURE 6.1 Mill-and-Inlay Thickness vs. Pavement Service Life (Based on Rutting Depth)**

## Chapter 7

### Prediction of Mill-and-Inlay Pavement Functional Life

#### 7.1 Introduction

One of the objectives of the mill-and-inlay approach is to improve the ride quality or serviceability of existing pavements. The functional life of a mill-and-inlay pavement can be computed from two different approaches. The first approach using the AASHTO equation would need cumulative number of 18-kip ESAL's, subgrade resilient modulus, structural number, reliability and overall standard deviation as inputs. Then, the change of serviceability or  $\Delta$ PSI can be computed. In the other approach, the serviceability (PSI) value at any time can be computed from the roughness measurement (e.g., International Roughness Index) using a regression equation.

#### 7.2 Computation of Structural Number

Nondestructive deflection testing (NDT) is an extremely valuable and rapidly developing technology. According to the 1993 AASHTO Pavement Design Guide, the NDT method of pavement structural number determination follows an assumption that the structural capacity of the pavement is a function of its total thickness and overall stiffness. The relationship between the effective structural number of the existing pavement ( $SN_{eff}$ ), thickness, and stiffness is:

$$SN_{eff} = 0.0045D\sqrt[3]{E_p} \quad (\text{Equation 7-1})$$

where:  $D$  = total thickness of all pavement layers above subgrade, inches; and

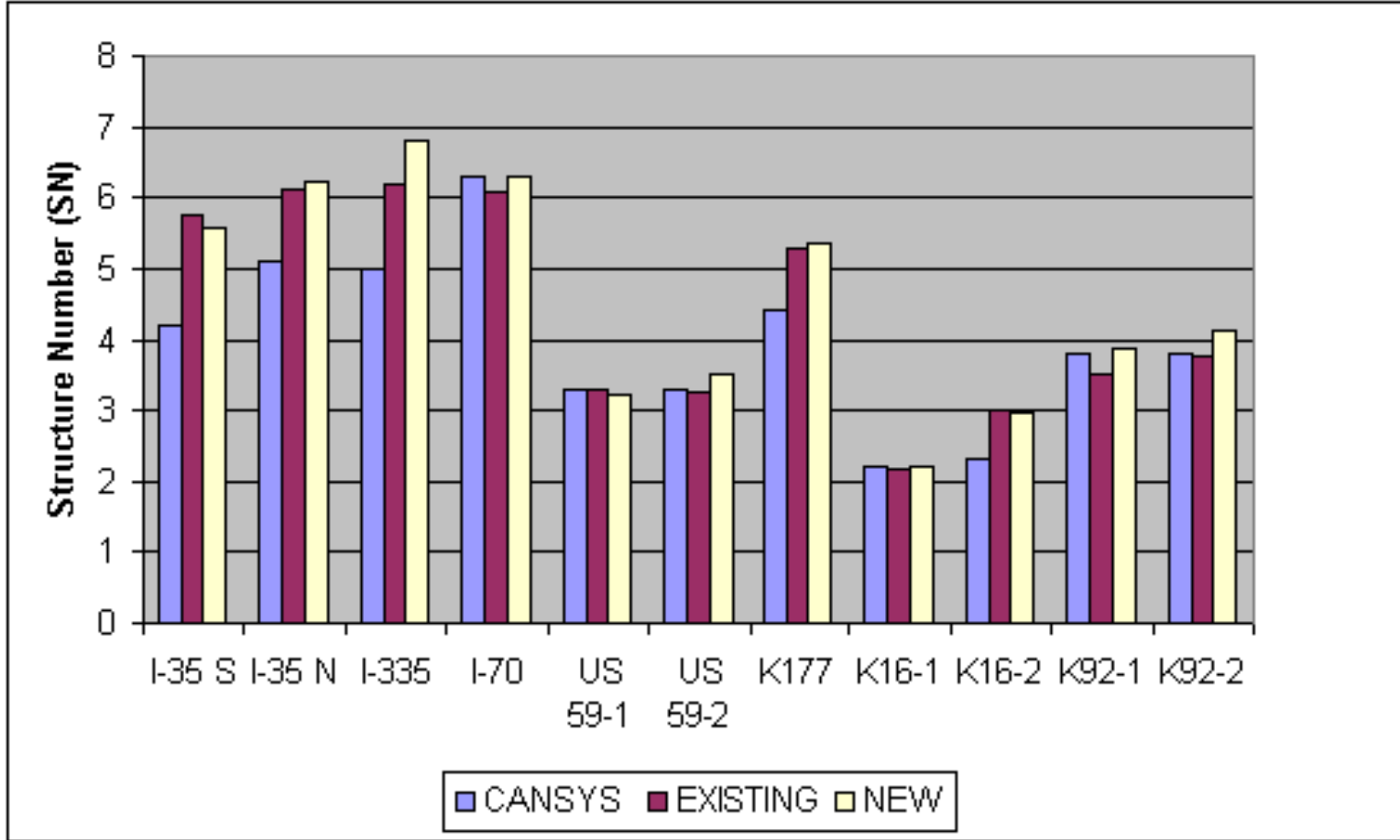
$E_p$  = effective modulus of the pavement layers above subgrade, psi.

Table 7.1 shows the calculated values of  $E_p$  and  $SN_{eff}$ . The values of  $E_p$  were backcalculated from the FWD data according to the procedure described in 1993 AASHTO Guide.

**TABLE 7.1 Calculated Values of  $E_p$  and  $SN_{eff}$  of the Test Sections**

No	Section	$E_p(kPa)$			$SN_{eff}$			CANSYS SN
		Existing	Milled	Inlay	Existing	Milled	Inlay	
1	I-35S	657,995	470,174	599,154	5.76	4.69	5.58	4.20
2	I-35N	877,786	626,301	928,428	6.11	5.05	6.22	5.10
3	I-335	992,160	775,125	1,364,220	6.21	5.01	6.80	5.00
4	US-59-1	1,581,255	2,019,804	1,481,350	3.31	3.29	3.24	3.30
5	US-59-2	1,516,489	2,563,080	1,910,597	3.26	3.24	3.52	3.30
6	K-16-1	2,266,465	2,445,950	1,556,451	2.17	1.91	2.19	2.20
7	K-16-2	602,186	2,583,750	4,661,085	3.01	1.79	2.96	2.30
8	K-92-1	1,330,046	651,518	1,770,386	3.51	2.56	3.86	3.80
9	K-92-2	1,629,141	482,197	2,181,374	3.76	2.13	4.14	3.80
10	K-177	1,506,154	322,108	1,570,093	5.29	2.19	5.36	4.40

Figure 7.1 shows the comparison of structural numbers (SN) from CANSYS database of KDOT (design or as-built values) and the calculated values from Equation (7-1) before (existing) and after inlay (new). Most of these values are equal or close to each other especially for KDOT pavements with low traffic volumes (US-59, K-16 and K-92). However, for high traffic pavement sections (K-177, I-35 and I-335), all values from CANSYS were lower than backcalculated values (existing and new). This is mainly because of frequent inlays/overlays done on those high traffic pavement sections over the years.



**FIGURE 7.1 Comparison of SN Values**

### 7.3 Analysis of Serviceability Loss

As mentioned earlier, two different methods were used to determine the loss of the pavement serviceability index ( $\Delta PSI$ ) to assess the functional life of mill-and-inlay pavement. The first one is the AASHTO equation and the other is the HPMS equation. It is to be noted that PSI is not necessarily the correct measure of performance when the pavement structure is concerned. However, since the mill-and-inlay strategy is frequently applied to improve the PSI value, the serviceability loss study would indicate whether traffic alone is the real indicator of PSI or not. In other words, the lives of the mill-and-inlay strategies from both fatigue and functional viewpoints can be compared.

#### 7.3.1 AASHTO Equation

The AASHTO equation is:

$$\log_{10}(W_{18}) = Z_R * S_o + 9.36 * \log_{10}(SN + 1) \quad (\text{Equation 7-2})$$

$$\frac{\log_{10} \left[ \frac{\Delta PSI}{4.2 - 1.5} \right]}{-0.40 + \frac{1094}{(SN + 1)^{5.19}}}$$

$$0.20 + 2.32 * \log_{10}(M_R) - 8.07$$

where:  $W_{18}$  = predicted number of 18-kip equivalent single axle load applications,

$Z_R$  = standard normal deviate;

$S_o$  = combined standard error of the traffic prediction and performance prediction;

$\Delta PSI$  = difference between the initial design serviceability index,  $p_o$ , and the design terminal serviceability index,  $p_t$ ; and

$M_R$  = resilient modulus (psi).

In Equation 7-2, all parameters are known for a mill-and-inlay pavement, thus  $\Delta$ PSI can be determined for a given number of 18-kip ESALs ( $W_{18}$ ). In this study, this value was taken as the cumulative 18-kip ESALs since last rehabilitation. Table 7.2 tabulates the  $\Delta$ PSI values for the mill-and-inlaid pavements since the last rehabilitation. The computed  $\Delta$ PSI are much smaller than the design loss in PSI values for most of the pavements. For new overlay design, the design  $\Delta$ PSI value is assumed to about 1.7 [= (4.2-2.5)] for the pavements on the primary network and 2.2 [= (4.2-2.0)] for the secondary pavements. The discrepancy between the actual loss in PSI and design PSI loss is greater for the low-traffic pavements, K-16-2 and K-92, as shown in Figure 7.2.

### **7.3.2 HPMS Equation**

The HPMS equation given by FHWA relates serviceability of a pavement to its measured roughness as shown below:

$$PSI = 5.0e^{-0.0041IRI} \quad \text{(Equation 7-3)}$$

where: IRI is international roughness index (in/mile).

The IRI values for each test section was collected before mill-and-inlay procedure from the Kansas pavement management system (PMS) database. Using Equation 7-3, the PSI values at the end of the service life of the pavement were calculated. Similarly, the initial PSI was calculated on each section from the measured IRI immediately after last rehabilitation. The difference of these two PSI values is the  $\Delta$ PSI for that section computed from the HPMS equation. Table 7.3 also tabulates these values. A comparison of these values with the AASHTO values indicate that the HPMS values are closer to the design values of  $\Delta$ PSIs assumed in the AASHTO overlay design procedure



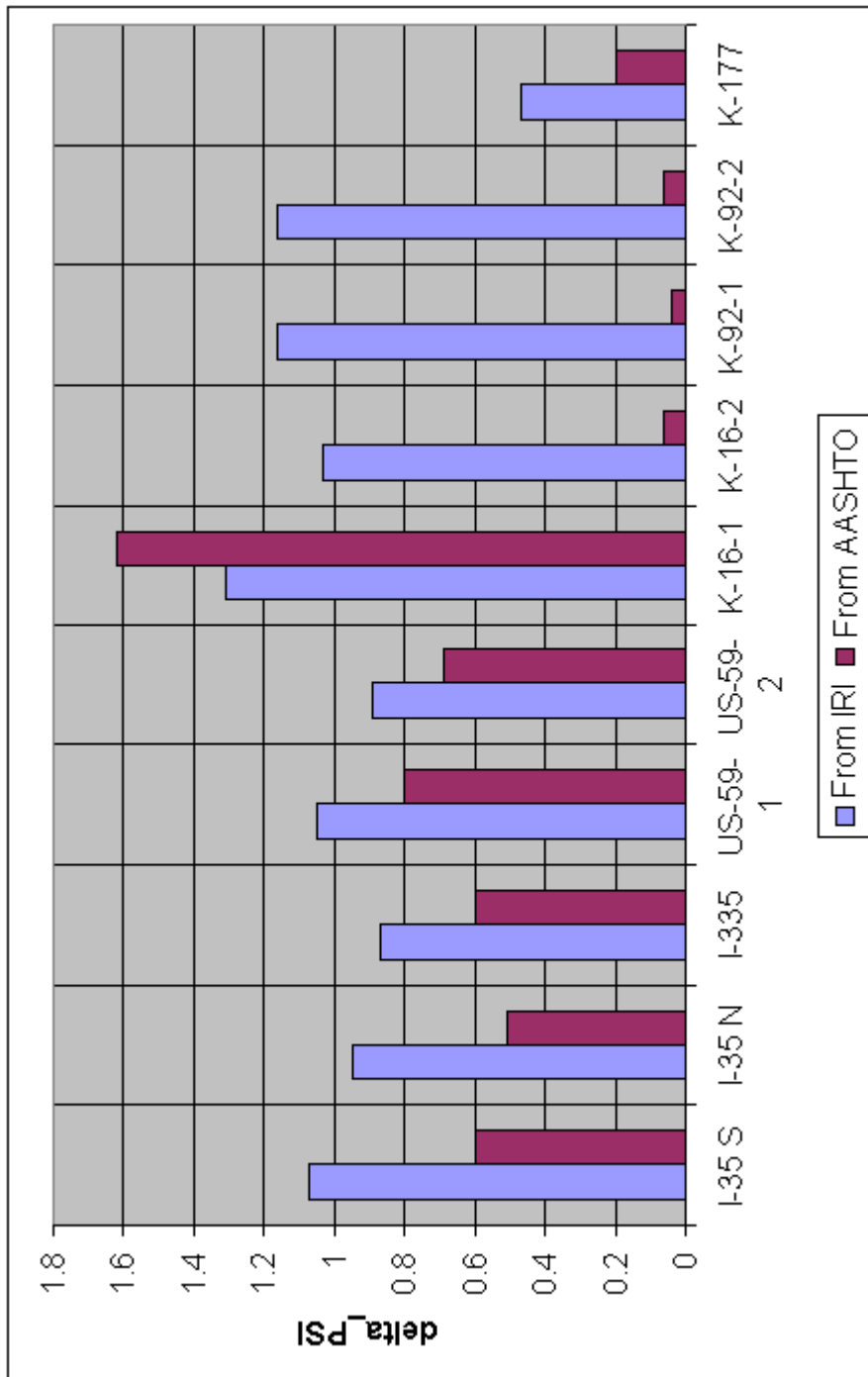


**FIGURE 7.2 Comparison of Serviceability Loss**

**TABLE 7.2 Calculated  $\Delta$ PSI Values from the AASHTO Equation**

<b>No</b>	<b>Section</b>	<b>So</b>	<b>R</b>	<b>Zr</b>	<b>W18</b>	<b>SN</b>	<b>Mr (MPa)</b>	<b><math>\Delta</math>PSI</b>
<b>1</b>	I-35 S	0.45	0.95	-1.645	1,881,875	5.76	151.6	0.60
<b>2</b>	I-35 N	0.45	0.95	-1.645	1,901,376	6.11	151.6	0.51
<b>3</b>	I-335	0.45	0.95	-1.645	1,405,070	6.20	108.2	0.60
<b>4</b>	US-59-1	0.45	0.75	-0.674	163,515	3.31	86.8	0.80
<b>5</b>	US-59-2	0.45	0.75	-0.674	166,085	3.26	96.5	0.69
<b>6</b>	K-16-1	0.45	0.60	-0.253	28,954	3.17	73.1	1.62
<b>7</b>	K-16-2	0.45	0.60	-0.253	19,056	3.01	88.3	0.06
<b>8</b>	K-92-1	0.45	0.60	-0.253	27,251	3.51	133.7	0.04
<b>9</b>	K-92-2	0.45	0.60	-0.253	27,251	3.76	122.0	0.06
<b>10</b>	K-177	0.45	0.75	-0.674	173,832	5.29	117.8	0.20

**TABLE 7.3 Comparison of  $\Delta$ PSI from the AASHTO and HPMS Equations**

No	Section	IRI <sub>init</sub> ( m/km)	IRI <sub>termi</sub> ( m/km)	Avg. IRI ( m/km)	PSI <sub>init</sub>	PSI <sub>termi</sub>	$\Delta$ PSI by HPMS	$\Delta$ PSI by AASHTO
1	I-35 S	43	115	109	4.19	3.12	1.07	0.60
2	I-35 N	43	106	96	4.19	3.24	0.95	0.51
3	I-335	43	100	84	4.19	3.32	0.87	0.60
4	US-59-1	43	113	106	4.19	3.15	1.05	0.80
5	US-59-2	43	101	115	4.19	3.30	0.89	0.69
6	K-16-1	43	134	117	4.19	2.89	1.31	1.62
7	K-16-2	43	112	112	4.19	3.16	1.03	0.06
8	K-92-1	43	122	112	4.19	3.03	1.16	0.04
9	K-92-2	43	122	112	4.19	3.03	1.16	0.06
10	K-177	43	72	73	4.19	3.72	0.47	0.20

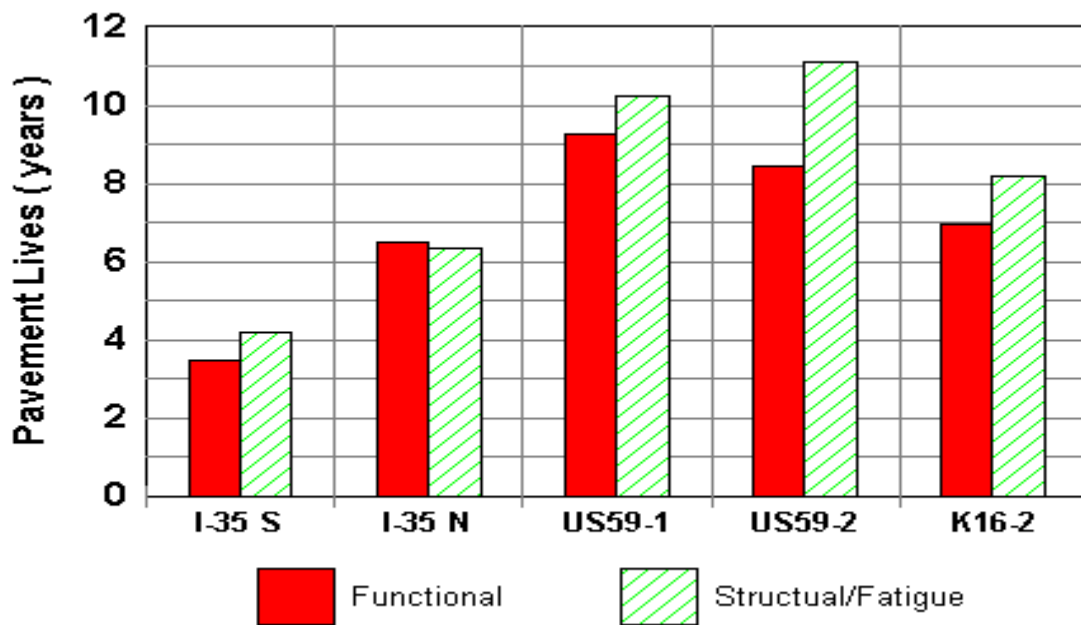
#### 7.4 Comparison of Service and Fatigue Lives

Figure 7.3 shows the functional lives predicted from the AASHTO equation and the fatigue lives predicted earlier from the fatigue equations for the sites on I-35, US-59, and K-16. The results show that the fatigue lives on most sections are usually equal to or more than the functional/service lives. This indicates that the pavement sections in this study will be rehabilitated mainly not due to pavement fatigue damage, but due to development of excessive roughness most likely from transverse cracking. Thus, on most mill-and-inlay pavements,

preservation of functional lives in terms of pavement surface roughness may be more critical than controlling pavement structural lives in terms of pavement fatigue damages.

### 7.5 Existing Pavement Damage

Existing pavement damage was assessed by comparing two critical pavement responses: (i) the horizontal tensile strain at the bottom of AC layer and (ii) the vertical compressive strain on the top of the subgrade before milling, after milling and after inlaying. Figures 7.3 thru 7.8 show these parameters for all pavement test sections corresponding to the 80 kN (18-kip) single-axle, dual tire load with a tire pressure of 690 kPa (100 psi). It is clear that both tensile strains and vertical strains increased significantly after milling. However, after inlaying, both strain values at least decreased to the pre-milling level, thereby indicating that the critical pavement responses remain unaffected due to the mill-and-inlay action.



**FIGURE 7.3 Comparison of Service and Fatigue Lives**

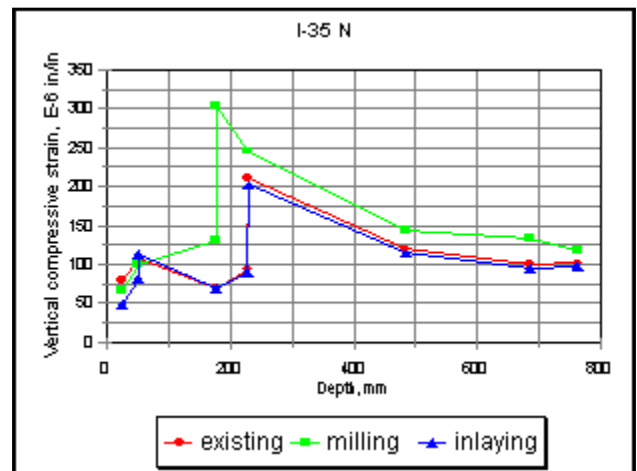
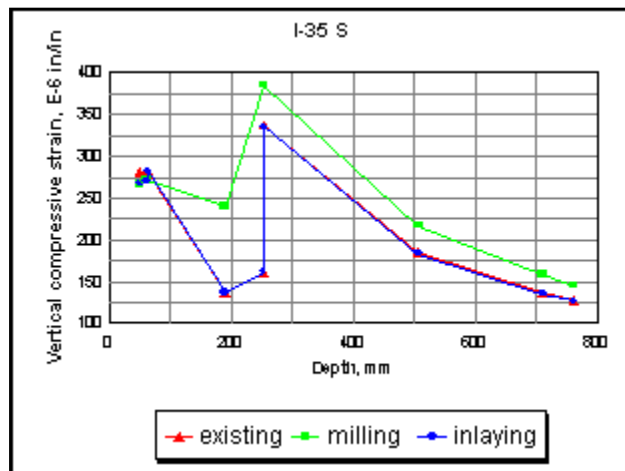
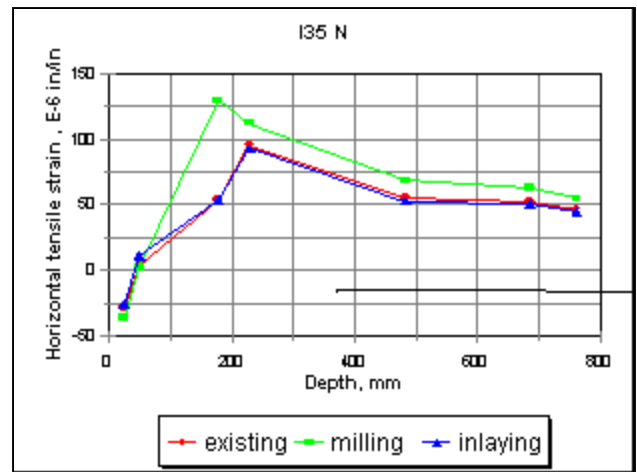
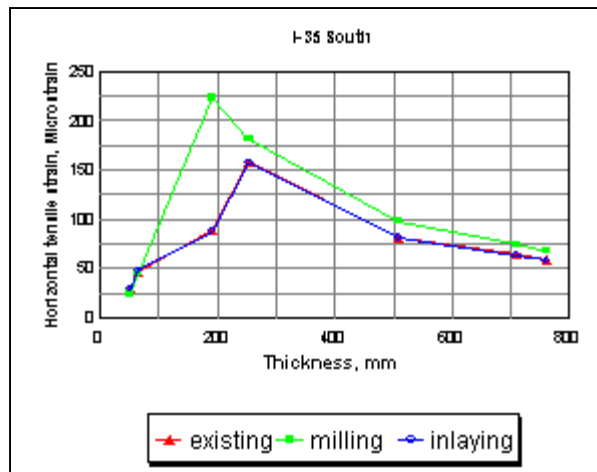


**FIGURE 7.4 Horizontal Tensile Strain and Vertical Compressive Strain for I-35 Sections**

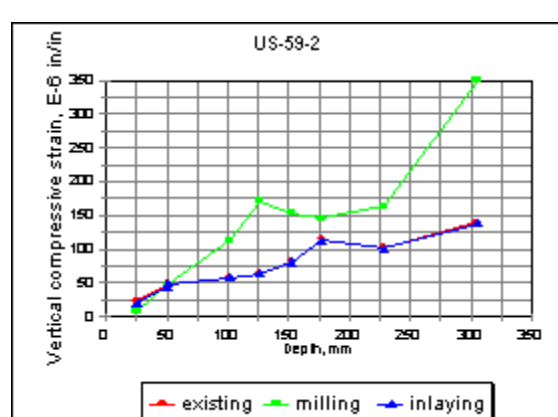
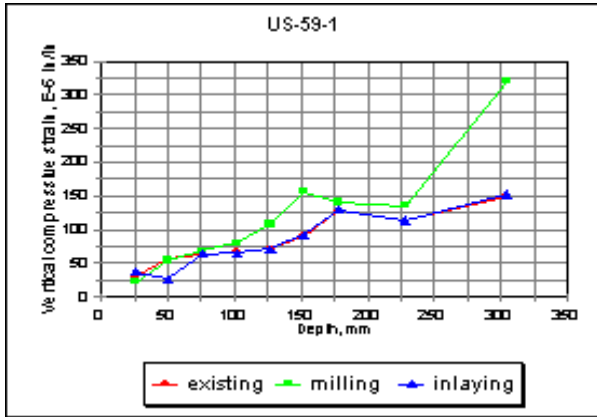
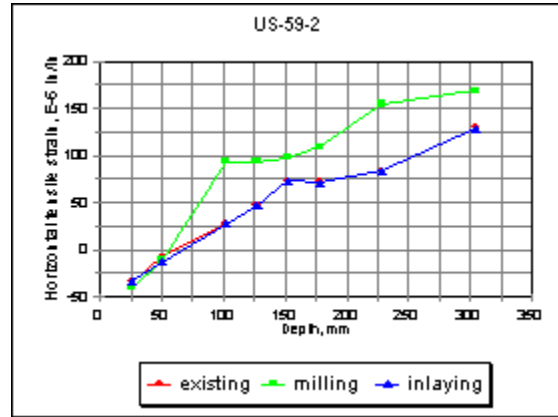
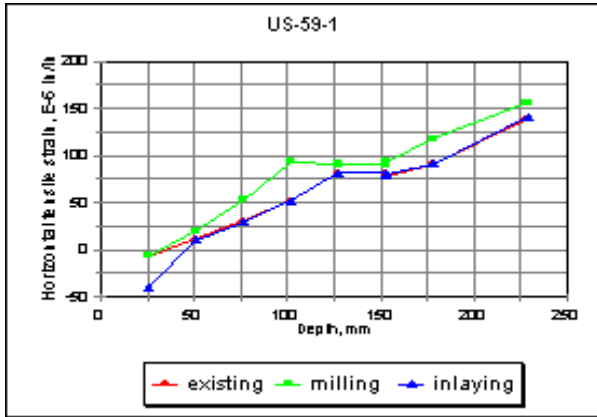


**FIGURE 7.5 Horizontal Tensile Strain and Vertical Compressive Strain for US-59 Sections**

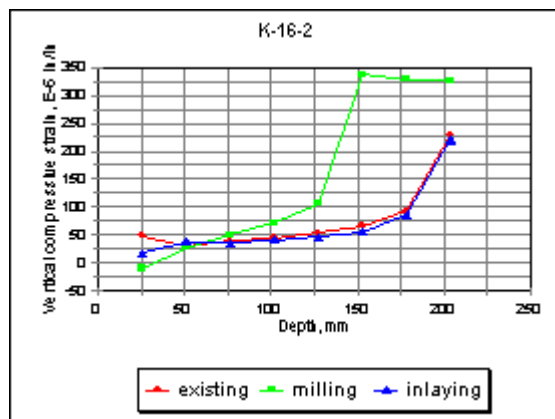
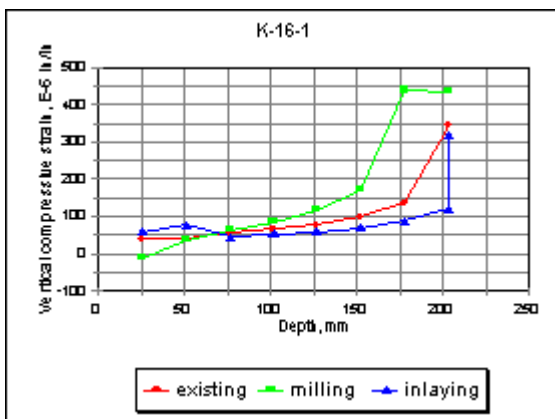
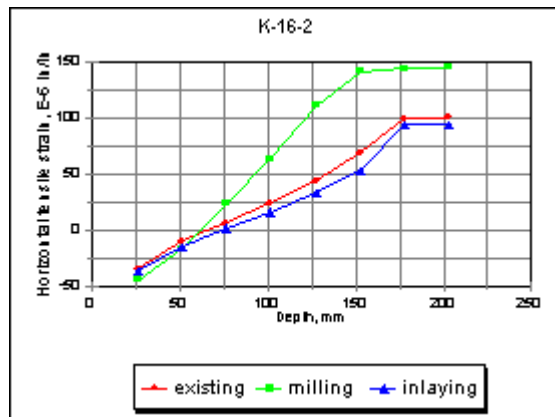
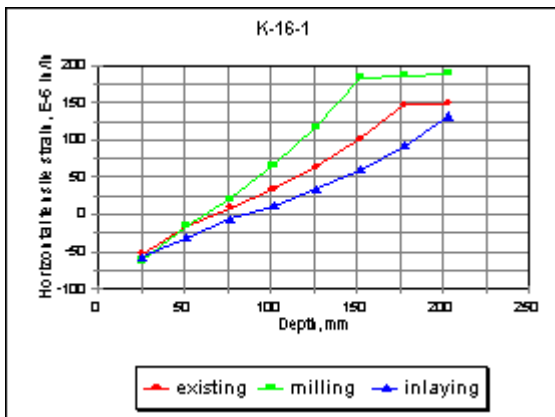


**FIGURE 7.6 Horizontal Tensile Strain and Vertical Compressive Strain for K-16 Sections**

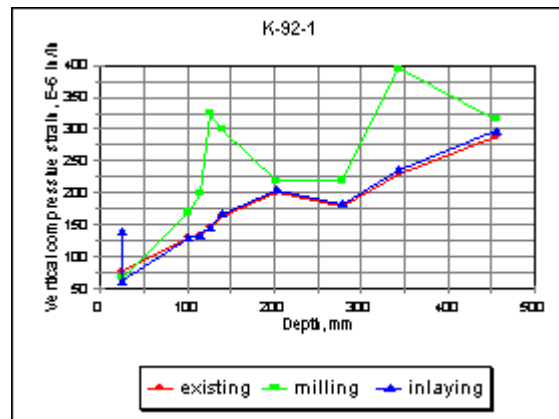
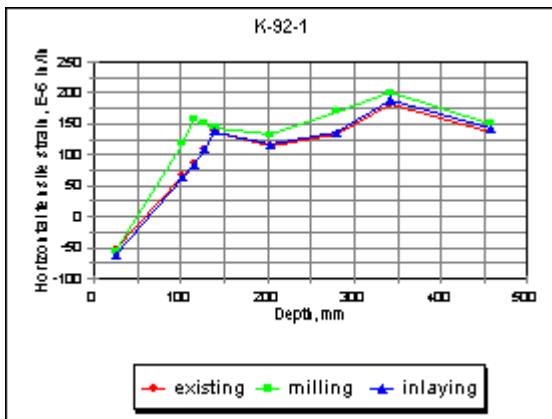
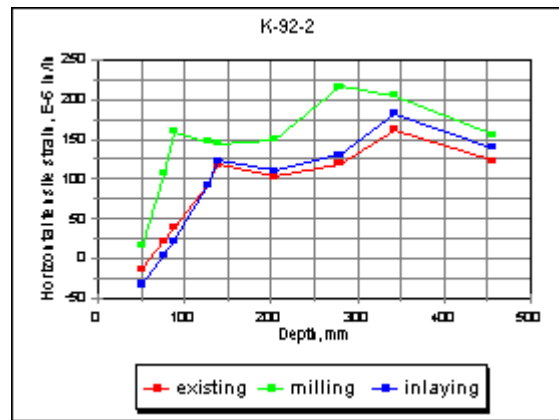
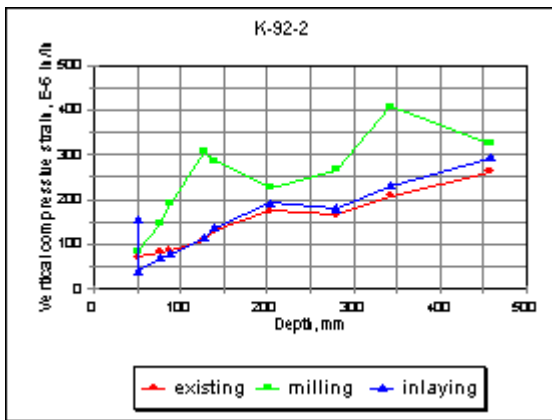


**FIGURE 7.7 Horizontal Tensile Strain and Vertical Compressive Strain for K-92 Sections**

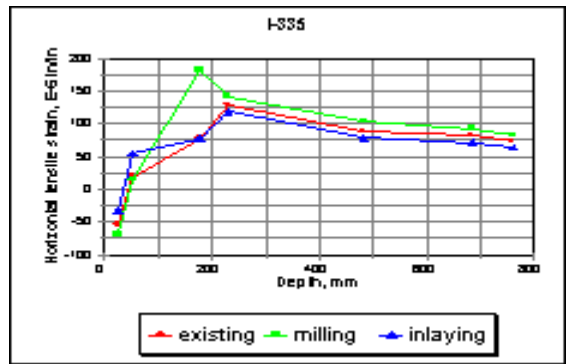
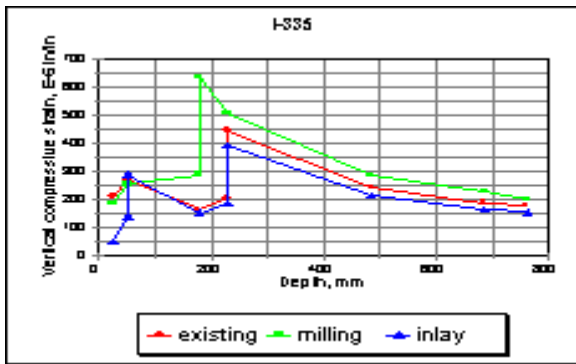
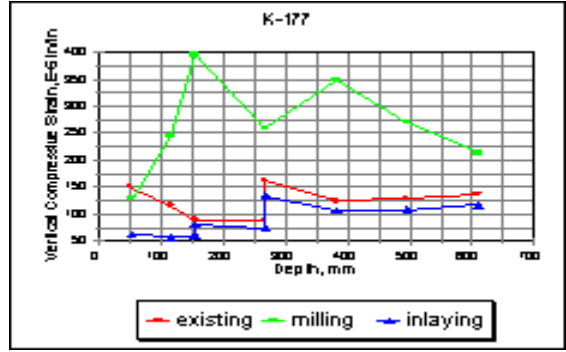
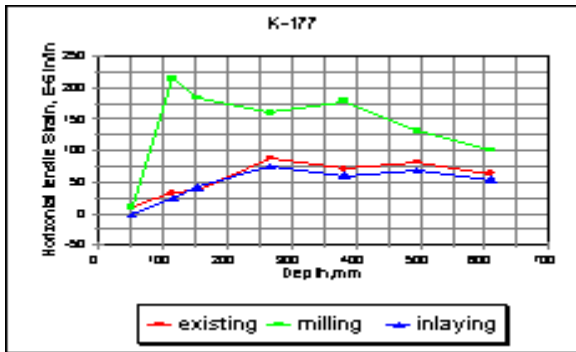


**FIGURE 7.8 Horizontal Tensile Strain and Vertical Compressive Strain for I-335 and K-177 Sections**

## Chapter 8

### Optimum Mill-and-Inlay Thickness Determination

#### 8.1 Introduction

On some major modification projects where deep milling is involved, KDOT currently selects a mill-and-inlay depth so that the ratio of this depth to the remaining milled pavement thickness would be higher than 1.0. This somewhat ensures that much of the full pavement thickness would consist of newer materials. This practice of KDOT was analyzed in this section.

#### 8.2 Sensitivity of the Mill-and-Inlay Pavement Thickness Based on Regression Equation

In order to study the effect of the mill-and-inlay thickness on pavement structural life, a multi-linear regression analysis was done where the tensile strain at bottom of the AC layer (before milling or after inlaying) was treated as a dependant variable and several independent variables were investigated. The independent variables included the ratio of the inlay thickness to the remaining pavement thickness, total pavement thickness above subgrade, ratio of the inlay layer modulus to the existing AC layer modulus, subgrade modulus, and effective modulus above subgrade,  $E_p$ . A linear equation was obtained using data from all sections except K-177. The data from K-177 was not included in the analysis since it had a much higher milling depth compared to other sections.

Excellent  $R^2$  value was obtained by including all five variables. However, the  $t$  values of the moduli ratio and total thickness above subgrade were too low implying that those two variables were not highly correlated with the independent variable. After dropping these two variables, the following equation was obtained:

$$\varepsilon_r = 21.55 * r_o - 0.03813E_p + 4.203M_r \quad (\text{Equation 8-1})$$

where:  $\varepsilon_r$  = horizontal tensile strain at bottom of the AC layer after inlaying or before milling,  $10^{-6}$  in/in;

$r_o$  = thickness ratio of inlay layer to the remaining milled AC layer;

$E_p$  = effective AC modulus above subgrade, ksi (backcalculated using the AASHTO algorithm); and

$M_r$  = subgrade modulus, ksi (backcalculated using the AASHTO algorithm).

The limitations of Equation 8-1 include a smaller database and possible auto-correlation of  $r_o$ ,  $E_p$ , and  $M_r$  with the horizontal tensile strain reason. Equation (8-1) was used to compute the horizontal tensile strains at the bottom of the AC layer for the I-35 South and US-59-1 sections for different thickness ratios. Figures 8.1 shows the relationships obtained. It appears that the fatigue lives of these pavements would be doubled by choosing thickness ratios of 1.25 for US-59 and 1.50 for I-35, respectively. Thus, it is apparent that in order to achieve a very high fatigue life, the mill-and-inlay thickness should be at least 1.25 times the thickness of the remaining AC layer. However, in some cases, the increase in thickness ratio may not significantly decrease the tensile strain at the bottom of the AC layer (or in other words, may not increase the fatigue life significantly) since it also depends on the existing pavement layer moduli.

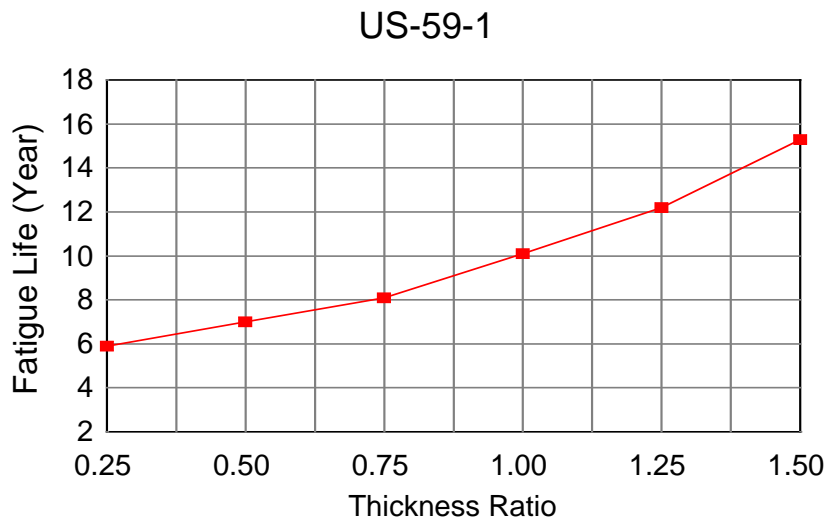
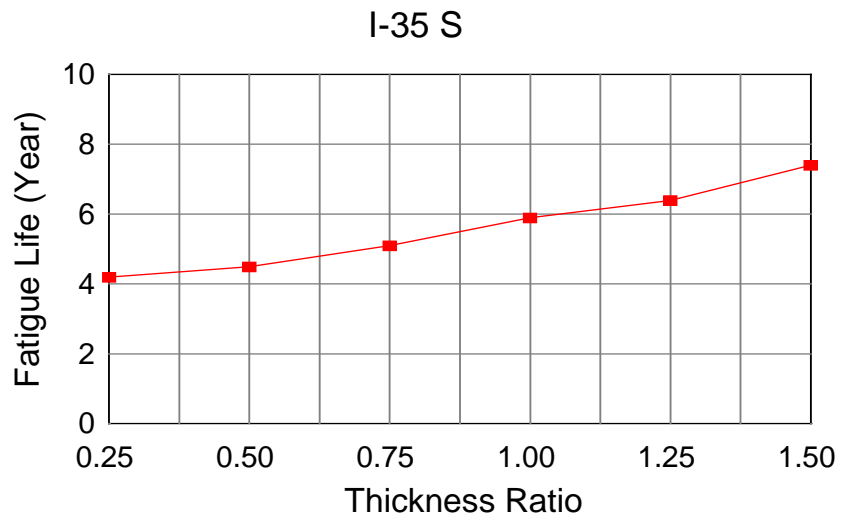


**FIGURE 8.1 Structural Live vs. Thickness Ratio**

### 8.3 Determination of the Mill-and-Inlay Thickness from the Equivalent Thickness Method

This methodology follows the recommendations for selecting of an overlay thickness in an “AASHTO Overlay Method Using NDT” as described in the Volume II, Appendix NN of the 1986 AASHTO Guide for Design of Pavement Structures (12). The overlay methodology proposed uses NDT testing to evaluate the in-situ deflection basin characteristics of the pavement and a backcalculation technique to estimate the elastic moduli ( $E_i$ ) of the pavement layers. Knowing the in-situ moduli, structural layer coefficients ( $a_i$ ) can then be employed that relate  $E_i$  to  $a_i$ . Knowledge of the structural coefficients ( $a_i$ ) of the existing in situ layers thus allows one to compute the effective number ( $SN_{eff}$ ) of the existing pavement from the following equation:

$$SN_{eff} = 0.0045 \sum h_i (E_i)^{1/3} \quad \text{(Equation 8-2)}$$

where:  $h_i$  = the thickness of the i-th layer above the subgrade; and

$E_i$  = the modulus of the i-th layer above the subgrade.

The overlay/inlay requirements can then be estimated by using the effective thickness concept. In this project, the “SN” in the KDOT CANSYS database has been taken as design “SN” for the pavement sections under study. The backcalculated moduli of the milled pavement and other layers (if any) were used to calculate the  $SN_{eff}$ . The deficiency in SN resulting from milling was calculated by subtracting  $SN_{eff}$ , determined from Equation 8-2, from the CANSYS SN. Finally, the inlay thickness was calculated by dividing the difference with 0.42, which is the structural layer coefficient of the new inlay AC material. It is to be noted that although the

CANSYS SN is calculated on the basis of algorithms based on the engineering judgement of degradation of the materials in different layers, it is only available SN which would be close to the actual design SN values of the existing pavements.

**TABLE 8.1 Computed Inlay Thicknesses by the Equivalent Thickness Method**

No	Section	CANSYS SN	Existing AC		BASE		$SN_{eff}$	Inlay Thickness (mm)
			$E_{AC}$ (MPa)	Thickness (mm)	$E_{AC}$ (MPa)	Thickness (mm)		
1	I-35 S	4.2	1,089	190.5	200	457.2	4.31	-7.6
2	I-35 N	5.1	2,308	177.8	234	457.2	4.81	17.8
3	I-335	5.0	1,543	177.8	138	457.2	5.20	-12.7
4	US-59-1	3.3	16,198	127	482	152.4	4.11	-45.7
5	US-59-2	3.3	23,109	101.6	220	152.4	3.55	-22.9
6	K-16-1	2.2	22,778	152.4	0	0.0	4.02	-15.2
7	K-16-2	2.3	39,900	139.7	0	0.0	4.44	-109.2
8	K-92-1	3.8	20,339	88.9	696	203.2	3.94	-129.5
9	K-92-2	3.8	4,361	114.3	634	203.2	3.36	-7.6
10	K-177	4.4	1,006	114.3	489	228.6	2.74	99.1

Table 8.1 tabulates the required inlay thicknesses for all pavement test sections in this study. The results obtained are mixed. There are no thickness requirements for I-35 South and I-335 for the given traffic whereas I-35 North sections requires about 1-inch overlay. The results

on US-59, K-16 and K-92-1 are very misleading presumably due to the very high existing AC moduli obtained in the backcalculation process. On K-177, 102 mm of inlay is required. Earlier analysis of this section showed that the fatigue life of this pavement would be the lowest at such an inlay depth. Thus, this procedure does not appear to be applicable to the mill-and-inlay pavements.

#### **8.4 Proposed Procedure for Selecting an Optimum Mill-and-Inlay Thickness**

Based on the results of this study, it appears that if the pavement shows no sign of fatigue cracking, the milling (and inlay) on such a pavement should be minimized. The highest milling depth selected may be taken to be equal to the highest rut depth observed on the section. If the pavement has fatigue cracks, the following steps are recommended to select an optimum mill-and-inlay thickness:

1. Collect historical traffic data on the design section since last rehabilitation and compute cumulative 18-kip ESAL's.
2. Collect FWD data and thickness history of the section.
3. Backcalculate the layer moduli using an algorithm based on the elastic layer theory. Apply appropriate temperature correction factors for the asphalt layer (s).
4. Calculate the maximum/critical horizontal tensile strain at the bottom of the existing AC layer ( $\epsilon_t$ ) using the backcalculated layer moduli.
5. Use the Asphalt Institute fatigue equation:

$$N_F = 0.0796 * (\epsilon_T)^{-3.291} * (E_{ac})^{-0.854} \quad \text{(Equation 8-2)}$$

( $E_{AC}$  is the backcalculated existing pavement AC modulus) to estimate the fatigue cycles to failure for different mill-and-inlay thicknesses. Assume an inlay layer modulus of 3.0 GPa (435,000 psi).

6. Construct an allowable ESAL's versus mill-and-inlay thickness curve, and select the optimum mill depth corresponding to the highest fatigue lives from this curve. Consider other distresses, like reflection cracking, if necessary and provide appropriate strategy, increased thickness, fabric reinforcement, etc.

## Chapter 9

### Conclusions and Recommendations

#### 9.1 Conclusions

Based on this study, the following conclusions can be drawn:

1. The fatigue lives of mill-and-inlay pavements may (i) increase, (ii) remain essentially unchanged, or (iii) decrease depending upon the modulus of the existing AC layer, modulus and thickness of the inlay layer, and presence or absence of fatigue-related distresses. For a fatigue-cracked pavement, if the existing pavement modulus is relatively small and lower than the inlay modulus, there would be a range of mill-and-inlay thickness at which higher fatigue life would be obtained. However, if the fatigue cracking is not present, milling would decrease the fatigue life of such a pavement. In case where such a pavement is milled very deep, the fatigue life would decrease up to a certain mill depth and then would increase.
2. The critical pavement responses remain unaffected due to the mill-and-inlay action indicating no damage of the underlying layers resulting from this practice.
3. The cost-effectiveness of the mill-and-inlay strategy in terms of cost/ESAL-mile is higher for pavements with higher traffic.
4. Fatigue lives of the pavements with very high AC moduli and asphalt base are fairly insensitive to the mill-and-inlay thickness.
5. Service lives of the pavements with respect to rutting appear to be insensitive to the mill-and-inlay thickness provided there are no mixture or construction-related

problems. In most cases, the service/functional lives and fatigue lives of the mill-and-inlay pavements are fairly close. However, in order to achieve significant gain in fatigue life, the mill-and-inlay thickness should be at least 1.25 times of the remaining AC layer thickness.

## **9.2 Recommendations**

The recommendations of this study are:

1. If the pavement shows no sign of fatigue cracking, the milling (and inlay) on such a pavement should be minimized, and the highest milling depth selected may be taken equal to the highest rut depth measured on that section. This appears to be applicable to most of the KDOT non-interstate pavements.
2. On Kansas Turnpike, the optimum mill-and-inlay thickness selected ranges from 50.8 to 76.2 mm, with 76.2 mm being the minimum thickness which should be chosen. However, the lives of these inlays would vary from 4 to 6 years indicating that the current practice should be continued at about 5 year intervals.
3. More precise mill-and-inlay thickness for the fatigue-cracked pavements should be selected based on the methodology proposed in this study.

## References

1. J.A Scherocman and W.M. Grant. Cold Planing and Recycling B and Economical Pavement Maintenance Technology. *Proceedings of the International Road Federation*. Vol. TS, 1981.
2. AASHTO. *Guide for Design of Pavement Structures*. American Association of State Highway and Transportation Officials, Washington, D.C., 1993.
3. Lukanen, E. *Temperature Adjustment for Backcalculated Asphalt Moduli*. Facsimile Memorandum received from Braun Intertec Corporation, July 1996.
4. Witczak, M.W. Design of Full Depth Asphalt Airfield Pavements. *Proceedings of the 3rd International Conference on the Structural Design of Asphalt Pavements*. Grosvenor House, London, England, Vol. 1, 1972, pp. 550-567.
5. Huang, Y.H. *Pavement Analysis and Design*. Prentice Hall, Englewood Cliffs, N.J., 1993.
6. Nunn, M.. Long Term Review. *Highways*, Croydon, London, England, January/February, 1998, pp. 11-13.
7. Hesham A. A. and S. D. Tayabji. *Mechanistic Evaluation of Test Data from LTPP Flexible Pavement Test Sections, Volume I: Final Report*. U.S. Department of Transportation, FHWA, April 1998, pp. 77-90.
8. *Comprehensive Truck Size and Weight (TS & W) Study: Phase I- Synthesis (Pavement and Truck Size and Weight Regulations) Working Paper 3*. Battelle Team, Columbus, Ohio, 1995
9. Hutchinson, B.G. and Haas, R. C. G. *Trade-Offs between Truck Transportation Costs and Infrastructure Damage Costs, Final Report*. Department of Civil Engineering, University of Waterloo, Waterloo, Ontario, 1994.
10. Deacon, J.A. *Pavement Wear Effect of Turner Trucks*. TRB Report. Transportation Research Board, National Research Council, Washington, D.C., 1988.
11. Ardani, A. *Rehabilitation of Rutted Asphalt Pavements, Project IR-25-3(96)*. Final Report, Colorado Department of Transportation, May 1993, pp.15-22.
12. AASHTO. *Guide for Design of Pavement Structures. Vol. 2*. American Association of State Highway and Transportation Officials, Washington, D.C., August 1986, pp. NN-1 - NN-7.

## **Appendix A**

### **Typical Asphalt Beam Photos**



PHOTO A1: Sawing of Field Beams

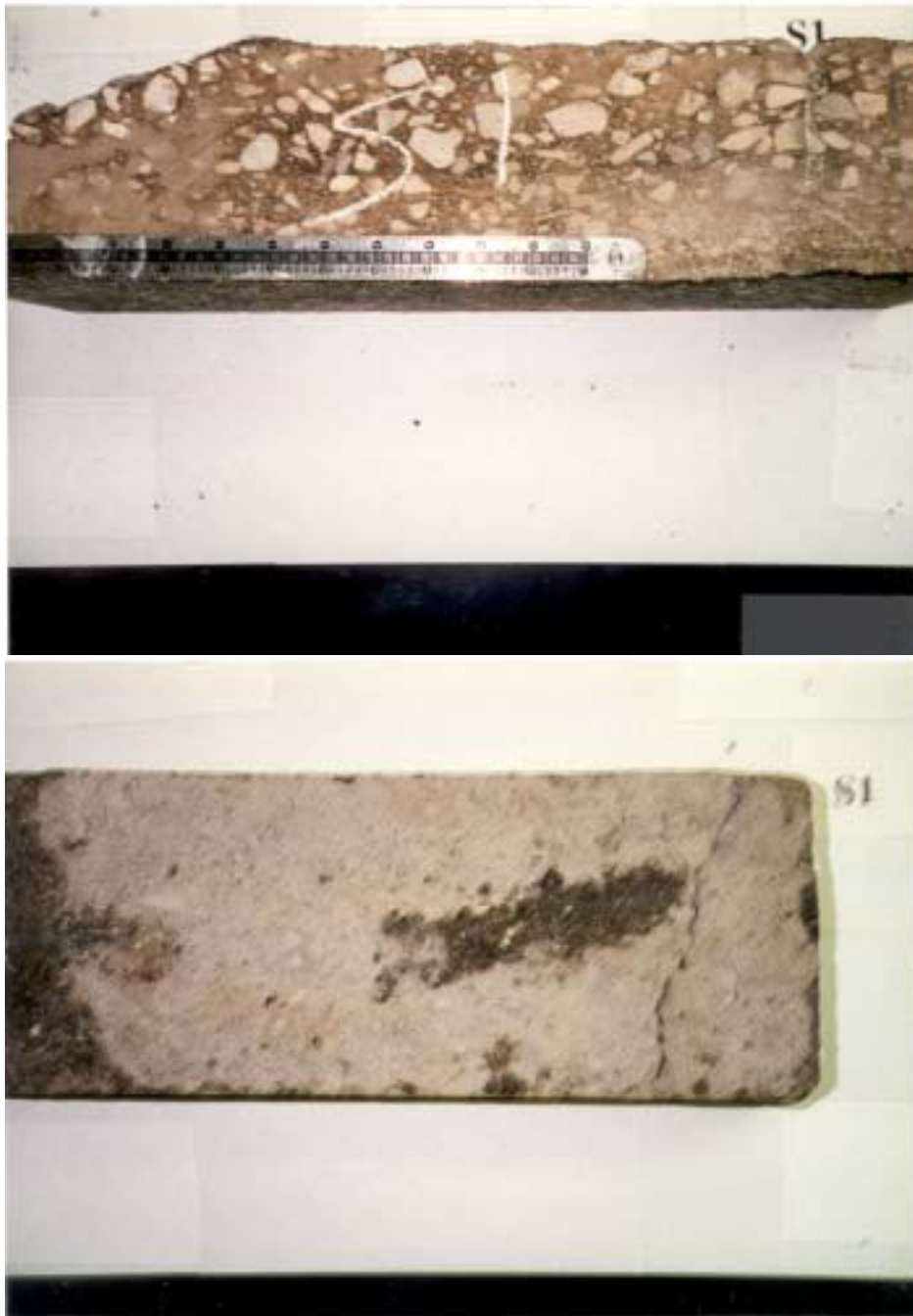


PHOTO A2: I-35 South Beams (Station I)

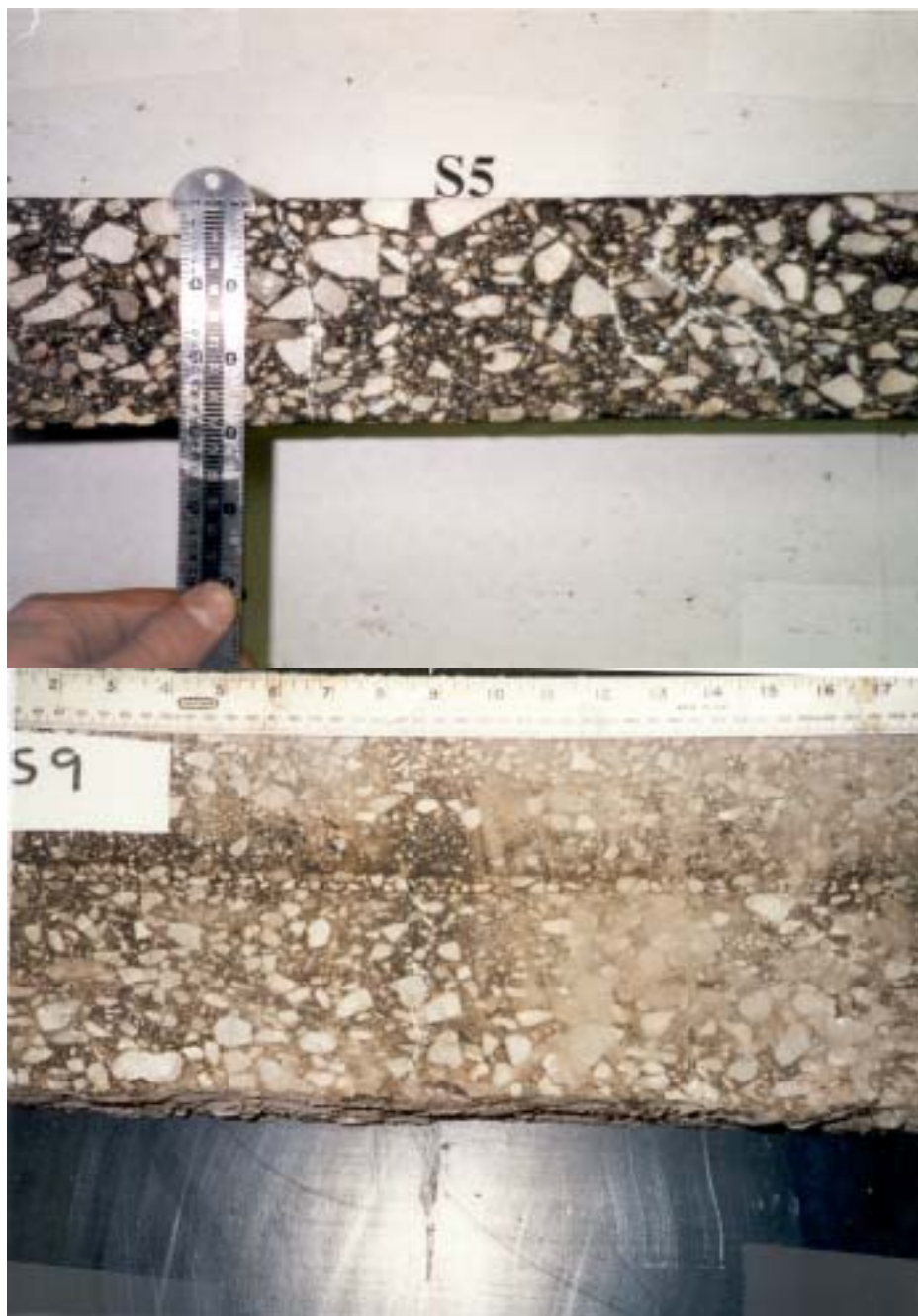


PHOTO A-3: I-35 South Beams (Station 9)

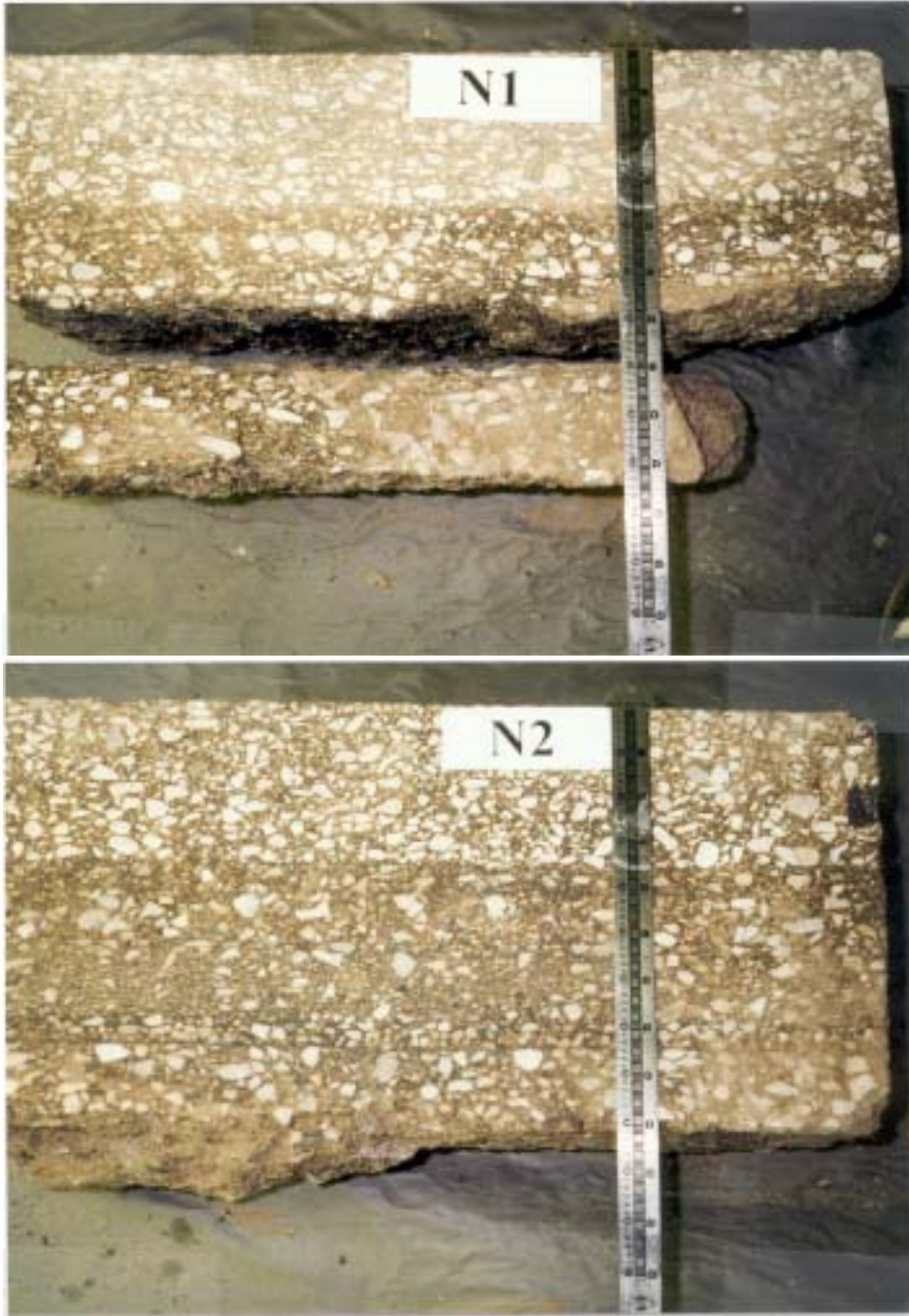


PHOTO A-4: I-35 North Beams (Stations 1 and 2)



PHOTO A-5: I-35 North Beams (Stations 3 and 4)

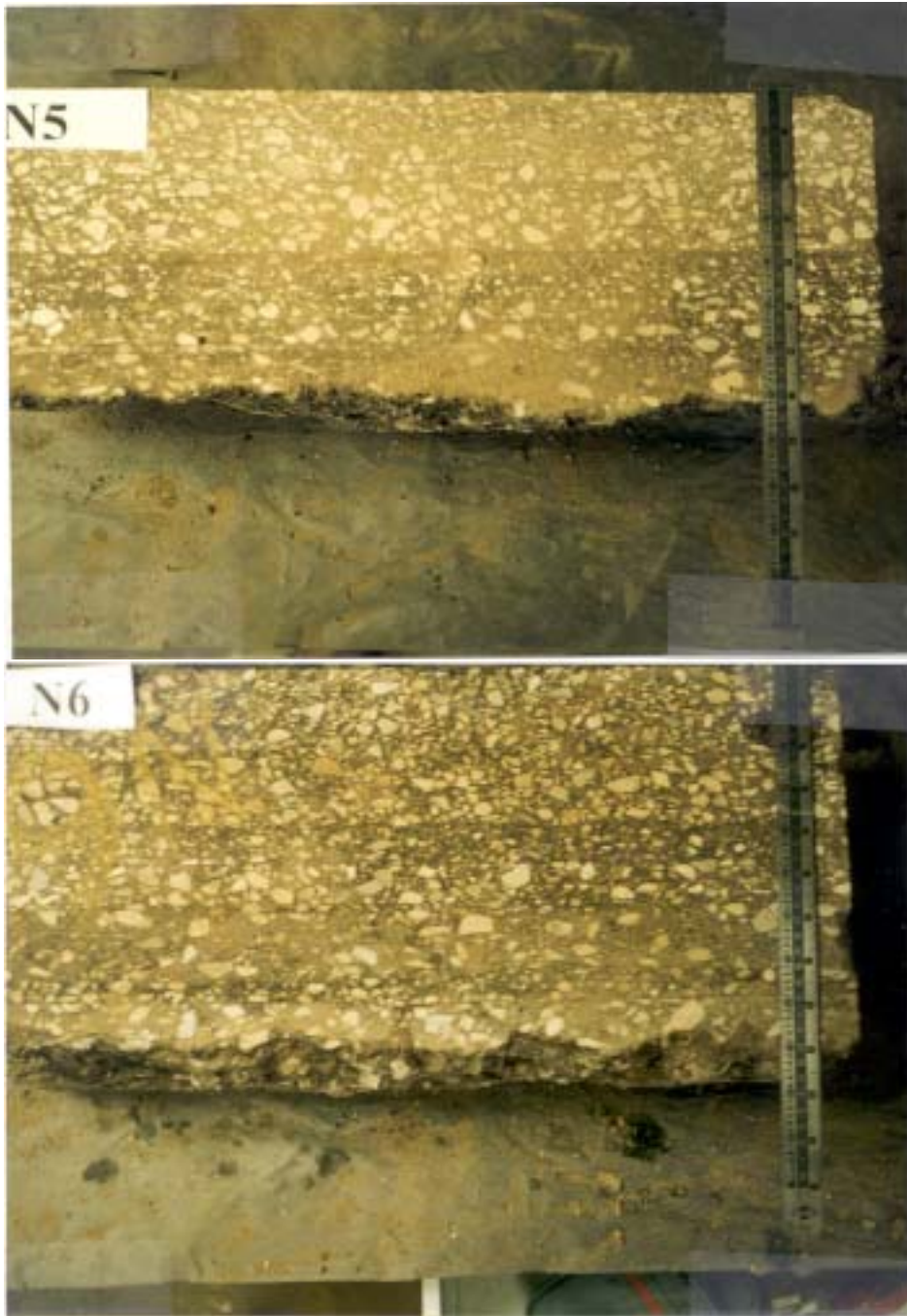


PHOTO A-6: I-35 North Beams (Stations 5 and 6)

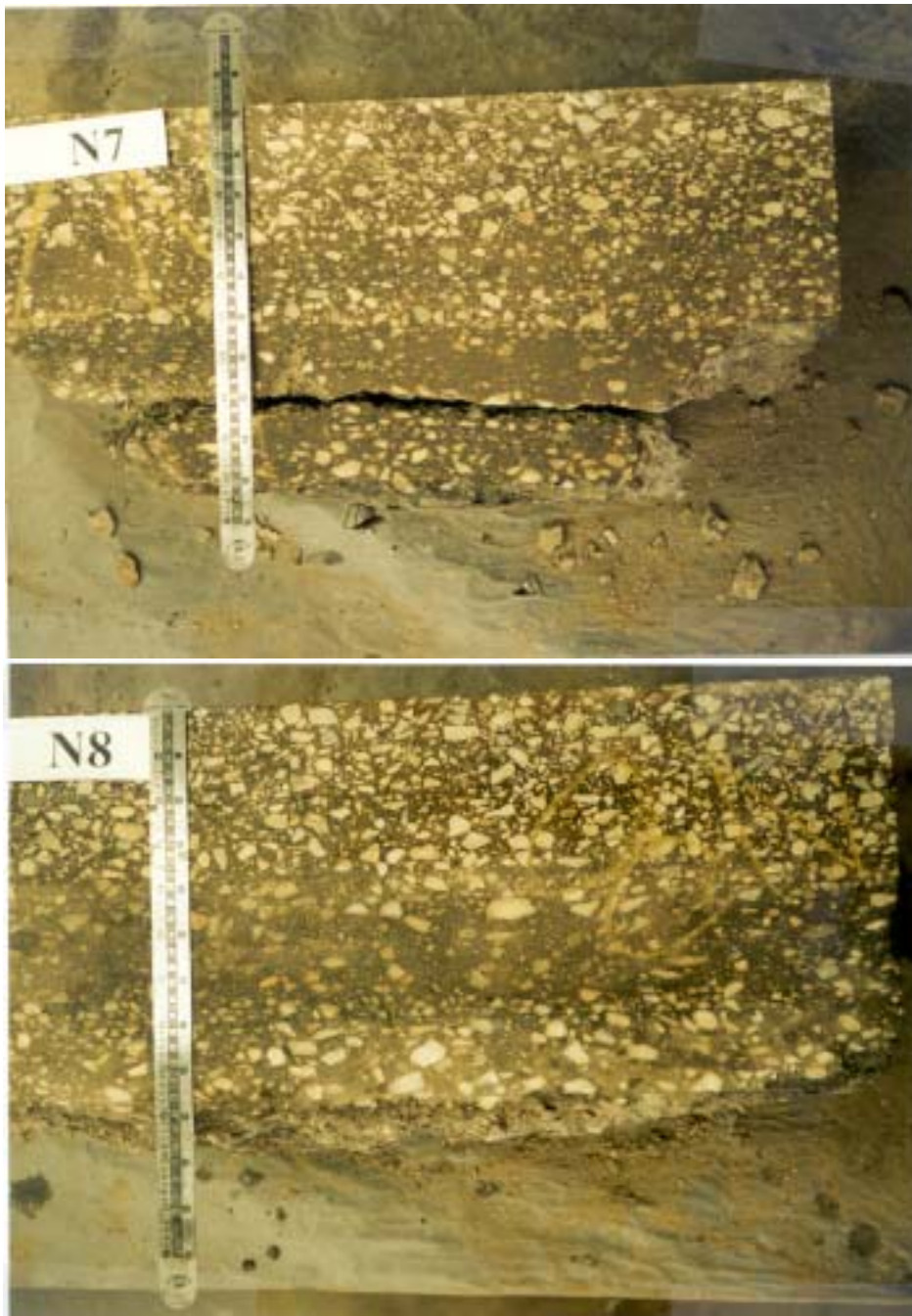


PHOTO A-7: I-35 North Beams (Stations 7 and 8)



PHOTO A-8: I-35 North Beams (Stations 9 and 10)



PHOTO A-9: K-16 Beams (Stations 100 and 200)

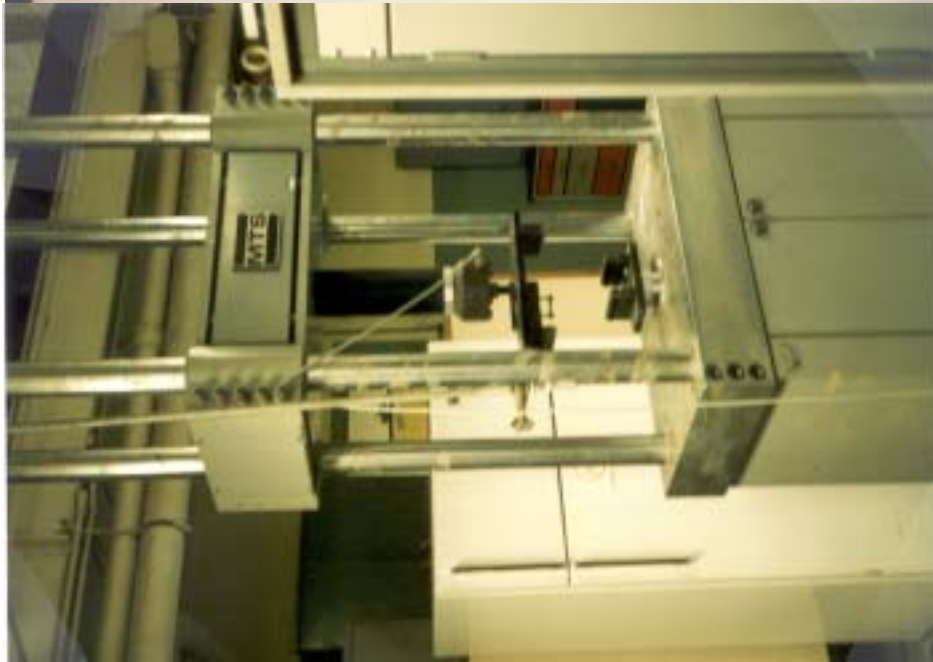
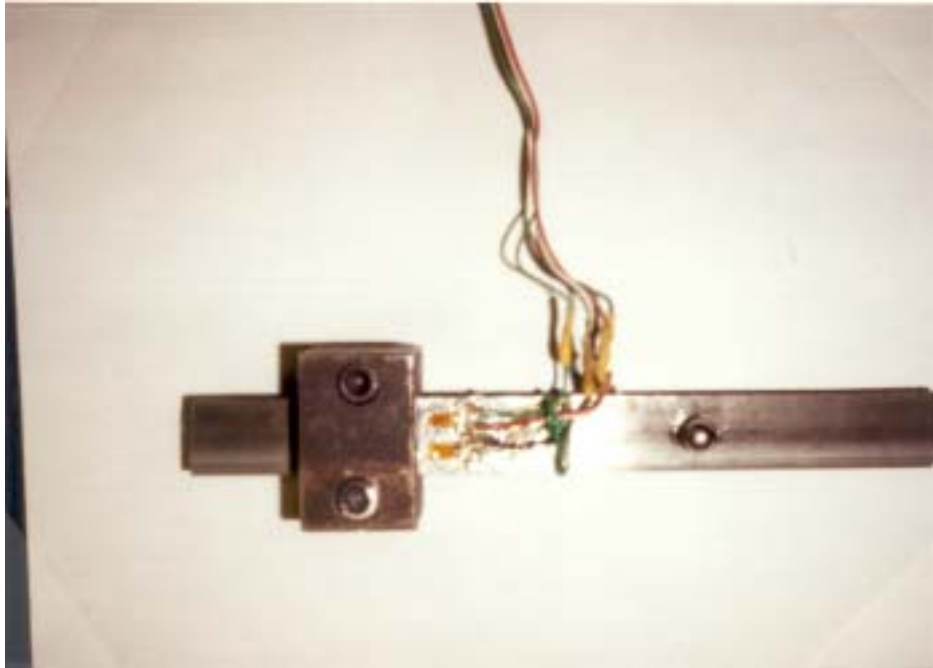


PHOTO A-10: Fatigue Test Setup

**APPENDIX B**  
**FATIGUE TEST RESULTS**

**Table B-1 Fatigue Test Results (I-35 S)**

Sample Name	length ( in. )	width ( in. )	height ( in. )	Load ( lbs )	Initial Modulus ( psi )	Initial Strain ( in./in.)	N f (cycles)	H of new (in.)
S1-new	16.0000	4.1458	3.0729	150	115895	0.00041	227168	1.50
S2-new	16.0625	4.1146	3.1146	1057	151245	0.00214	538	1.75
S3-new	16.0000	4.0260	3.1458	500	165942	0.00093	7302	1.50
S5-new	16.0000	4.1042	3.0833	600	159922	0.00118	11386	1.50
S6-new	16.0000	3.9792	3.0469	400	147824	0.00090	11147	1.25
S7-new	16.0000	4.0104	3.0208	700	140240	0.00167	1345	2.00
S8-new	16.0625	4.0833	3.0625	794	114503	0.00222	145	1.75
S9-new	16.0625	4.0938	3.0938	529	163872	0.00101	9763	2.50
MEAN					144552	0.001308		1.72
STDs					18955	0.000641		0.39
S1-base	16.0000	4.0938	3.1563	300	131335	0.00069	8191	/
S2-base	16.0625	3.9167	3.0625	529	214968	0.00082	652	/
S3-base	16.0625	4.0833	3.0729	400	206583	0.00062	5203	/
S6-base	16.0000	4.0417	3.0417	250	196206	0.00042	14459	/
MEAN					187273	0.00064		
STDs					38073	0.00017		

**Table B-2 . Fatigue Test Results (I-35 N)**

Sample Nam	length ( in. )	width ( in. )	height ( in. )	Load ( lbs )	Initial Modulus ( psi )	Initial Strain ( in./in.)	N f (cycles)	H of new (in.)
N1-new	16.000	4.1250	3.0000	500	163986	0.00102	3206	2.0
N2-new	16.000	4.1250	3.0833	400	112739	0.00110	5632	2.0
N3-new	16.000	3.9690	3.0210	400	212198	0.00063	6808	2.0
N4-new	16.750	4.1458	3.1771	300	147560	0.00059	16435	2.0
N5-new	16.125	4.1719	3.2135	350	158223	0.00063	23128	2.0
N6-new	16.000	4.0573	3.1354	350	124886	0.00086	14756	2.0
N7-new	16.125	4.1458	3.0729	300	123055	0.00076	16978	2.0
N8-new	16.000	4.0625	3.0938	300	140996	0.00067	30473	2.0
N9-new	16.000	4.0729	3.0938	425	188101	0.00071	5966	2.0
N10-new	15.950	4.0938	3.0365	250	204186	0.00040	73947	2.0
MEAN					157593	0.000737		
STDs					34601	0.000208		
N2-base	16.125	4.1042	3.0000	200	83878	0.00079	95435	/
N3-base	16.000	4.1250	3.0160	300	179964	0.00054	47905	/
N5-base	16.000	4.1458	2.7917	300	178495	0.00063	15429	/
N6-base	16.000	4.0417	3.0521	350	93740	0.00121	13809	/
N7-base	16.125	4.1042	3.1667	300	153986	0.00058	22652	/
N8-base	16.000	4.1042	2.8906	325	128955	0.00090	2960	/
N10base	16.000	4.0990	3.0990	250	176808	0.00044	58826	/
MEAN					176808	0.000727		
STDs					40836	0.000263		

**Table B-3 Fatigue Test Results (US-59-1)**

Sample Nam	length ( in. )	width ( in. )	height ( in. )	Load ( lbs )	Initial Modulus ( psi )	Initial Strain ( in./in.)	N f (cycles)	H of new (in.)
1-1-new	16.000	4.0000	3.1000	206.5	328,622	0.000199	55,412	1.0
1-2-new	16.000	4.0000	3.0000	295	124,543	0.000802	87,943	1.0
1-3-new	16.000	3.2500	3.0000	177	377,915	0.000195	100,276	1.0
1-4-new	15.900	4.0000	2.7000	177	213,967	0.000403	23,234	1.0
1-6-new	16.000	4.0000	3.0000	118	341,684	0.000127	122,440	1.0
1-7-new	16.000	4.1000	2.9800	147.5	149,727	0.000330	83,247	1.0
1-8-new	16.000	4.2000	3.1000	177	142,883	0.000409	25,179	1.0
MEAN					239,906	0.000352		
STDs					107,085	0.000226		
1-3-base	16.000	4.0000	3.0000	295	95,123	0.001050	1,170	/
1-4-base	16.000	4.1000	3.0000	236	226,253	0.000345	94,446	/
1-5-base	16.000	4.0000	3.0000	206.5	58,035	0.001205	7,120	/
1-8-base	16.000	4.1000	3.1000	206.5	114,736	0.000557	6,386	/
MEAN					123,537	0.000789		
STDs					72,401	0.000405		

**Table B-4 Fatigue Test Results (US-59-2)**

Sample Nam	length ( in. )	width ( in. )	height ( in. )	Load ( lbs )	Initial Modulus ( psi )	Initial Strain ( in./in. )	N f (cycles)	H of new (in.)
2-1-new	16.000	4.1000	3.0000	80	182,070	0.000145	36,541	2.0
2-2-new	16.000	3.9500	3.0000	100	297,272	0.000115	31,954	2.0
2-3-new	16.000	4.0000	3.0500	105	169,174	0.000203	34,810	2.0
2-4-new	16.750	4.1000	2.9000	130	62,899	0.000731	24,288	2.0
2-5-new	16.125	4.1000	3.0500	130	69,285	0.000600	35,898	2.0
2-6-new	16.000	4.1000	3.0000	110	194,758	0.000187	93,434	2.0
2-7-new	16.125	4.1000	3.1000	75	198,783	0.000177	61,577	2.0
2-8-new	16.000	4.1300	3.1000	90	61,013	0.000453	157,480	2.0
MEAN					166,567	0.000326		
STDs					82,717	0.000236		
2-2-base	16.125	4.1000	2.9500	75	116,412	0.000220	15,070	/
2-3-base	16.000	4.1000	2.9500	75	138,113	0.000185	25,307	/
2-4-base	16.000	4.1000	2.8500	90	135,128	0.000244	4,097	/
2-5-base	16.000	4.1000	3.0000	70	97,224	0.000238	15,307	/
2-6-base	16.125	4.1000	2.9000	60	81,892	0.000259	8,735	/
2-7-base	16.000	4.1000	2.9500	60	156,466	0.000131	14,777	/
MEAN					120,873	0.000213		
STDs					27,806	0.000047		

**Table B-5 Fatigue Test Results (K-16-2)**

Sample Nam	length ( in. )	width ( in. )	height ( in. )	Load ( lbs )	Initial Modulus ( psi )	Initial Strain ( in./in. )	N f (cycles)	H of new (in.)
3-1-new	16.125	4.0000	2.8750	265.5	197,294	0.000496	20,879	2.0
3-3-new	16.000	4.0000	3.2000	265.5	176,125	0.000449	18,153	2.0
3-4-new	16.000	4.1000	2.9000	236.0	163,374	0.000511	8,569	2.0
3-5-new	16.000	4.0000	3.0630	88.5	123,480	0.000223	53,429	2.0
MEAN					165,068	0.000420		
STDs					31,055	0.000134		
3-1-base	16.125	4.0000	3.0000	206.5	99,444	0.000703	63,151	/
3-2-base	16.000	3.9000	2.9500	206.5	176,521	0.000406	6,911	/
3-3-base	15.900	4.1000	3.0000	206.5	106,179	0.000642	109,148	/
3-4-base	16.000	3.8000	3.0000	265.5	177,412	0.000533	10,189	/
MEAN					139,889	0.000571		
STDs					42,903	0.000013		